Skeletonization and Its Application to Quantitative Morphometry

Punam Kumar Saha
Professor
Departments of ECE and Radiology
University of Iowa

THE IOWA INSTITUTE FOR
BIOMEDICAL IMAGING

Overview of Our Research

- Overall Objective: Quantitative characterization of local properties of structure geometry, topology, and scale
- Specific Aims: To go beyond material content measures
  - Quantitative characterization of architecture and topology
  - Geometric and topologic separation and classification of structures
  - Relationship among structural properties, disease, intervention and genotypes

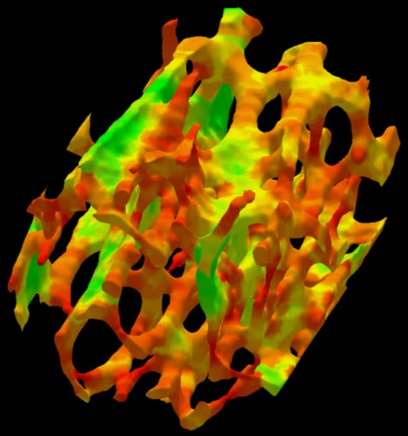

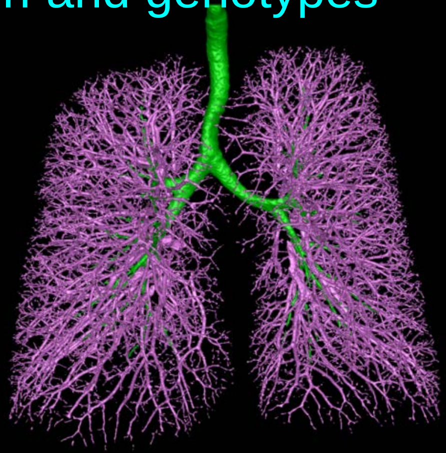

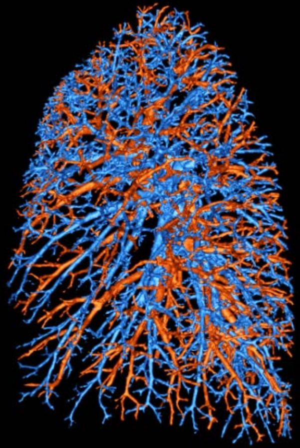

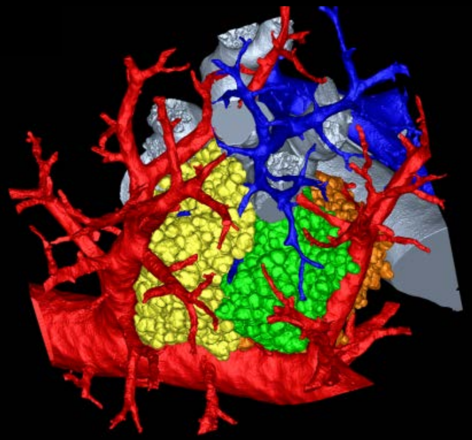

Outline

- Skeletonization
  - Fuzzy Skeletonization
- Applications of Digital Topology and Geometry in Object Characterization

Outline

- Skeletonization
- Applications of Digital Topology and Geometry in Object Characterization

Principle of Skeletonization

- Object: A closed and bounded subset of R^n
- Maximal Included Ball: A ball included in the object that cannot be cannot be fully included by another ball inside the object
- Skeleton: Loci of the centers of maximal included balls

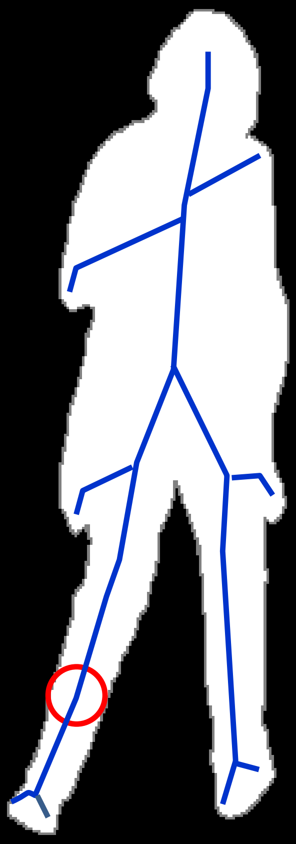

Basic Advantages of Skeletonization

- Dimensionality Reduction: Reduces the dimension of an object under consideration
  - A 2D object is reduced to a set of 1D curves
  - A 3D object is reduced to a set of 2D surfaces and 1D curve
- A Compact yet Sufficient Representation: Useful in many low- as well as high-level image related tasks including object representation, retrieval, manipulation, matching, registration, tracking, recognition, compression etc

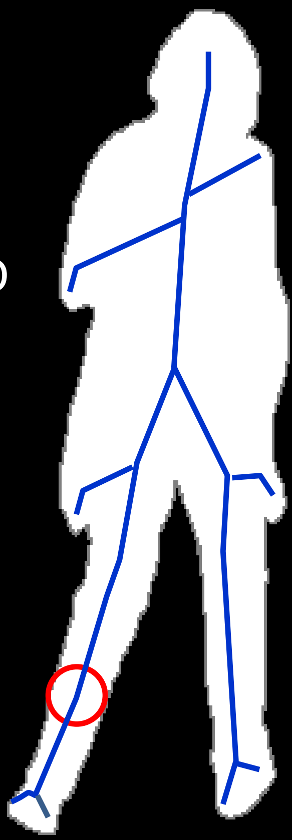

Basic Processes for Skeletonization

- Blum's Grassfire Transform
- Maximal Included Balls
- Enclosed Touching Balls

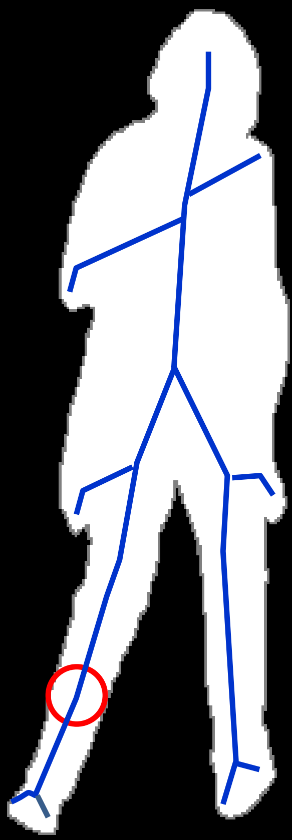

Blum’s Grassfire Propagation

- Blum’s grassfire transform is defined by fire propagation on a grass field, where the field resembles a binary object
  - grassfire is simultaneously initiated at all boundary points
  - grassfire propagates inwardly at a uniform speed
  - the skeleton is defined as the set of quench points where two or more opposite fire fronts meet

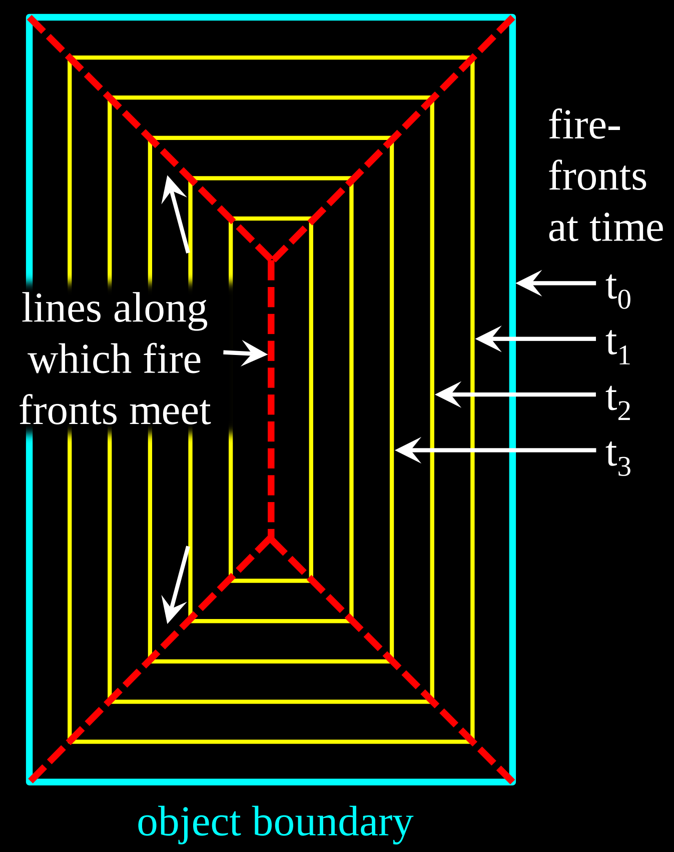

Maximal Included Balls

- The skeleton of an object is defined as the loci of the centers of maximal included balls

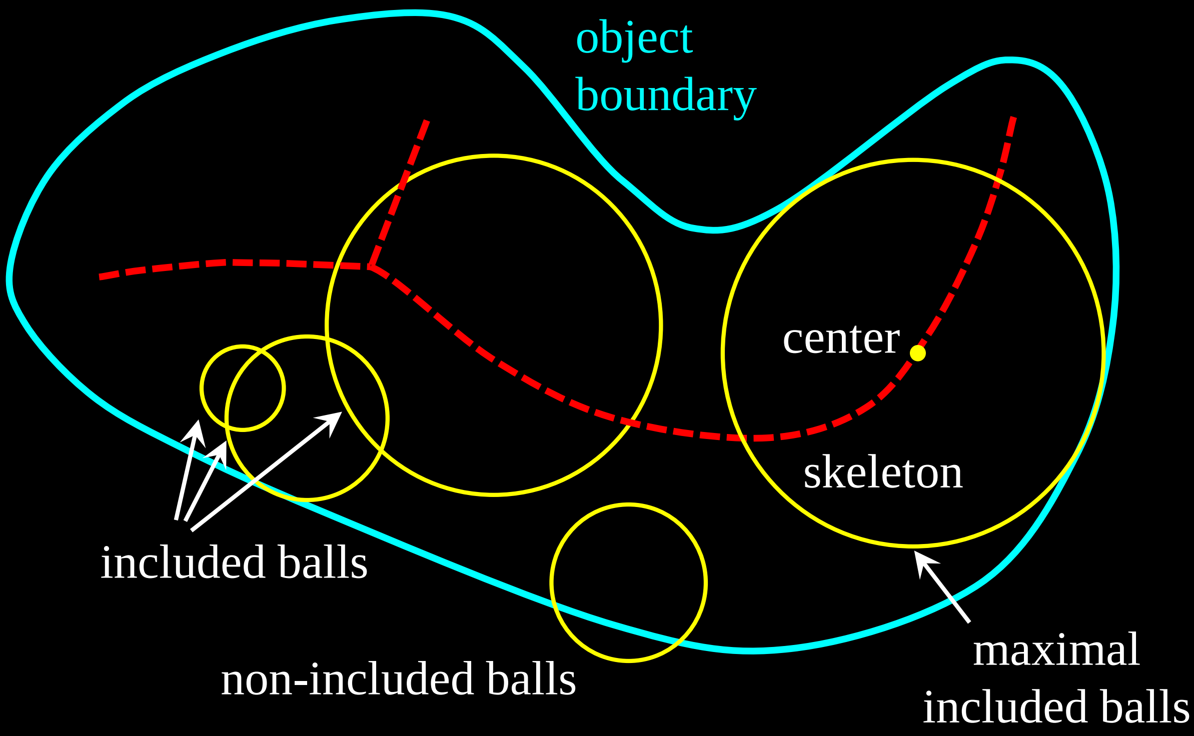

Enclosed Touching Balls

- The skeleton of an object is defined as the loci of the centers of enclosed balls touching the object boundary at two or more disjoint locations

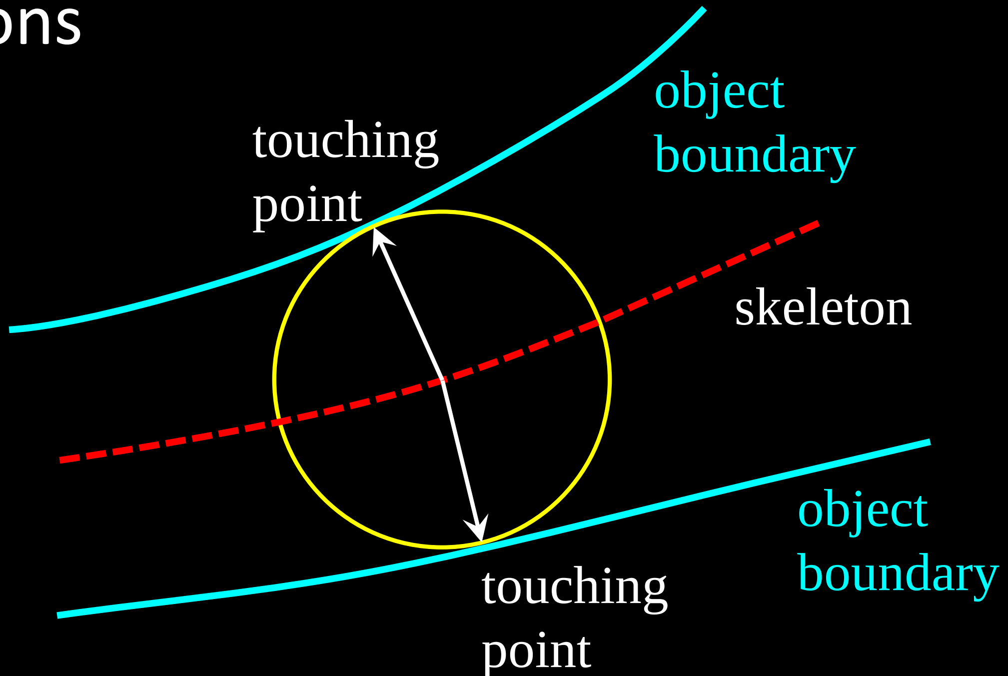

Skeletonization of Digital Objects

- Despite the long and rich tradition of computing skeletons of digital objects from the 1960s onward we are NOT AGREED on definitions, notations or evaluation process

- Intuitively, a skeleton should ideally have the following properties
  - It should have the same topology as the object, i.e., the same number of components, holes (and tunnels)
  - It should be thin
  - It should be centered within the object
  - It should preserve the geometric features of the objects
  - It should allow complete recovery of the original object

Different Approaches of Skeletonization

- The three basic processes of skeletonization are equivalent in a continuous space
- However, these processes generates different results for digital objects
- Skeletonization algorithms may be classified into three major categories based on their computational strategies and the underlying object representation
  - Geometric Approaches
  - Curve Propagation Approaches
  - Digital Approaches

Geometric Approaches

- The object boundary is represented by discrete sets of points in continuous space
  - point-clouds
  - polygonal (polyhedral) representations
- Algorithms are based on the Voronoi diagram or other continuous geometric approaches;
- Mostly, these algorithms use Voronoi edges (Voronoi planes) to locate the symmetry structures or the skeleton of an object

Voronoi Skeletonization

- The original object in the continuous space
- A polygonal representation by sampling vertex points on the object boundary
- The Voronoi diagram of sampled vertices is computed
- The Voronoi skeleton consist of the part of the Voronoi diagram that intersects the discrete object
- Skeletal segments “deep” inside the object consist of all segments that do not touch the boundary.

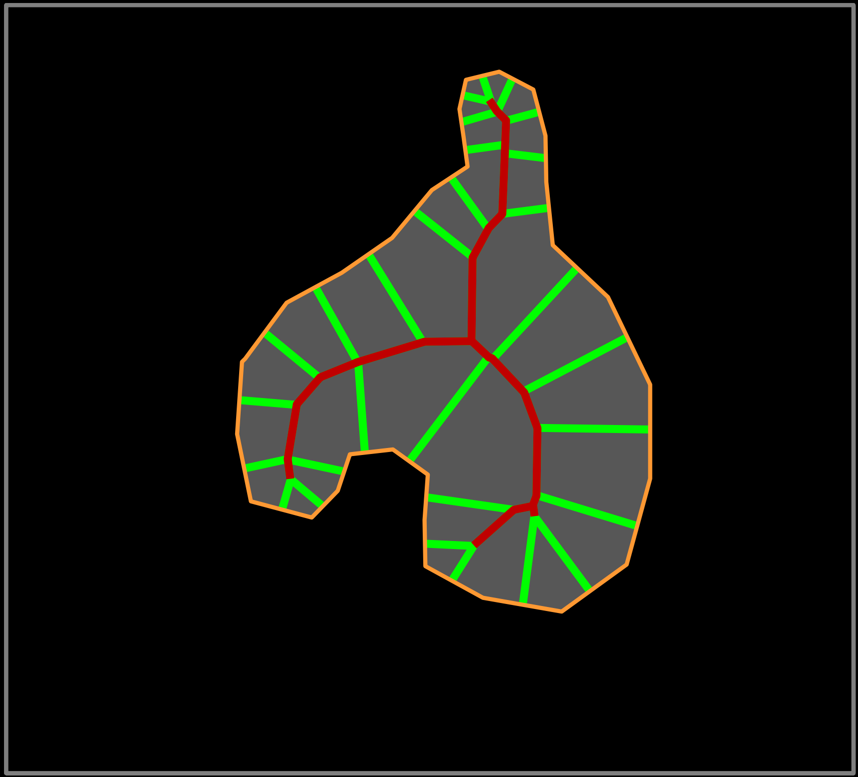

Curve Propagation Approaches

- The object boundary is represented by a continuous curve or a digital approximation of a continuous curve
- Algorithms are based on the principle of continuous curve evolution of the object boundary
- The symmetry structures or the skeleton are formed at singularity locations, specifically, at collision points of evolving curves.

Results: Curve Propagation Approaches

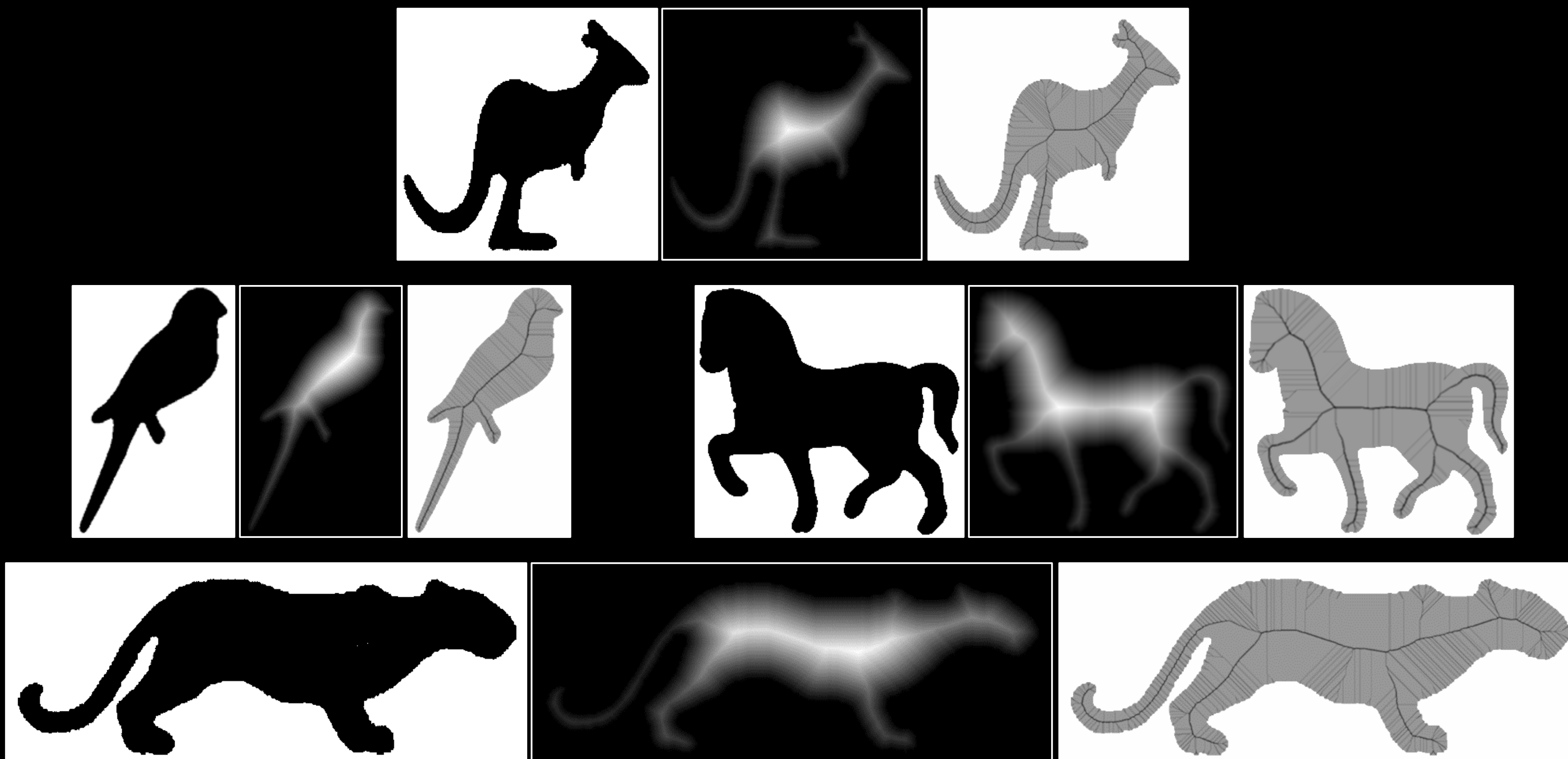

Digital Approaches

- The object is represented by a set of pixels (voxels) in a digital space
- Algorithms use the principle of digital morphological erosion or the location of singularities on a digital distance transform (DT) field to locate skeletal structures
- Often, such algorithms require explicit criteria for topology preservation.

Results: Digital Approaches

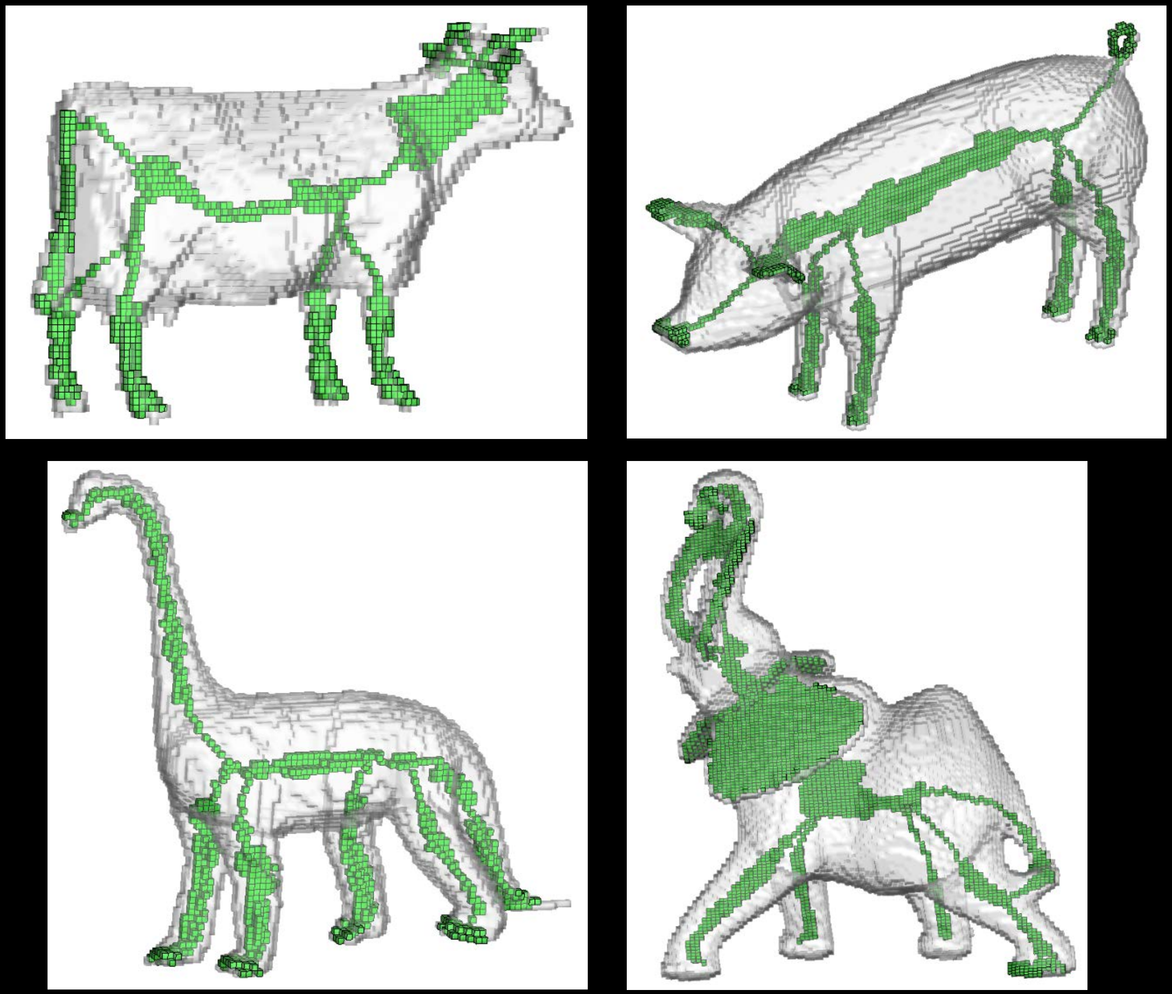

Outline

- Skeletonization
  - Fuzzy Skeletonization
- Applications of Digital Topology and Geometry in Object Characterization

Principle of Fuzzy Skeletonization

- Fuzzy Object: A membership value is assigned at each voxel
- The membership value is interpreted as the fraction of object occupancy in a given voxel or local material density
- Fuzzy Grassfire Propagation
  - grassfire is simultaneously initiated at the boundary of the support of a fuzzy object
  - the speed of fire-front at at given voxel is inversely proportion to its material density, i.e., membership value
  - grassfire stops at quench voxels when its natural speed of propagation is interrupted by colliding impulse from opposing fire-fronts

Outline of the Algorithm

- Primary skeletonization
  - Locate fuzzy quench voxels in the decreasing order of FDT values and filter those using local shape factor
  - Sequentially remove simple points that are not necessary for topology preservation in the increasing order of FDT values
- Final skeletonization
  - Convert two-voxel thick structures into single-voxel structures
  - Remove voxels with conflicting topological and geometric properties
- Skeleton pruning
  - Compute global shape factor to detect spurious branches
  - Delete spurious branches

Simple Points: Topology Preservation

Theorem: A point *p* is a 3-D simple point if and only if it satisfies the following four conditions:

- *p* has a black 26-neighbor
- *p* has a white 6-neighbore
- The set of black 26-neighbors of *p* is26-connected
- The set of white 6-neighbors of *p* is 6-connected in the set of white 18-neighbors of *p*

Simple Points: Examples

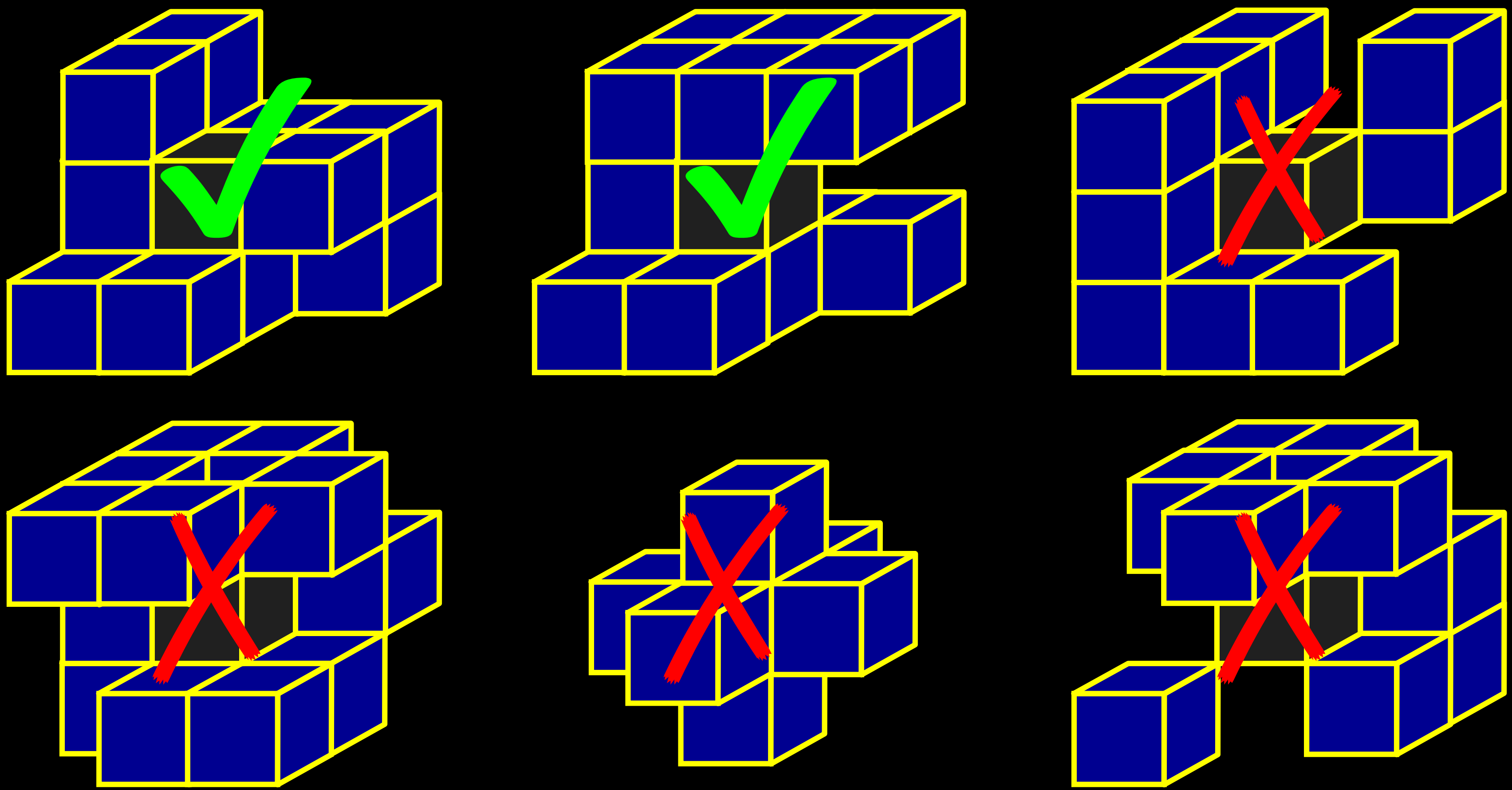

Fuzzy Quench Voxels

- During fuzzy grassfire propagation, the speed of a fire-front at a given voxel equates to the inverse of local material density
- Fuzzy distance transform defines the time when the fire-front reaches at a given voxel
- This process is violated only at quench points where the propagation is interrupted by colliding impulse from opposite fire-fronts

How to Define a Quench Voxel

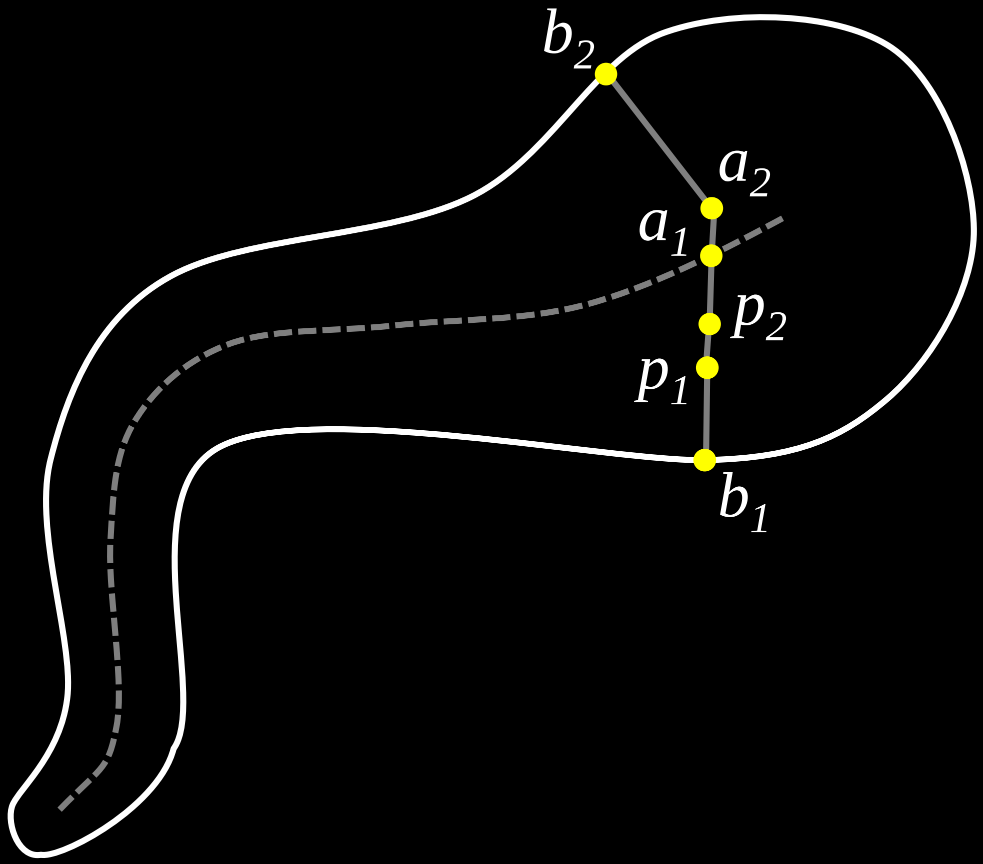

Definition of Quench Voxels

- A voxel *p* is a fuzzy quench voxel† in a fuzzy object if an only if the following inequality holds for every neighbor *q* of *p*

$$FDT(q) - FDT(p) < \frac{1}{2}\big(\mu_{\mathcal{O}}(p) + \mu_{\mathcal{O}}(q)\big)|p - q|^{\dagger}$$

- Fuzzy quench voxel is equivalent to center of maximal ball for binary digital objects

Examples

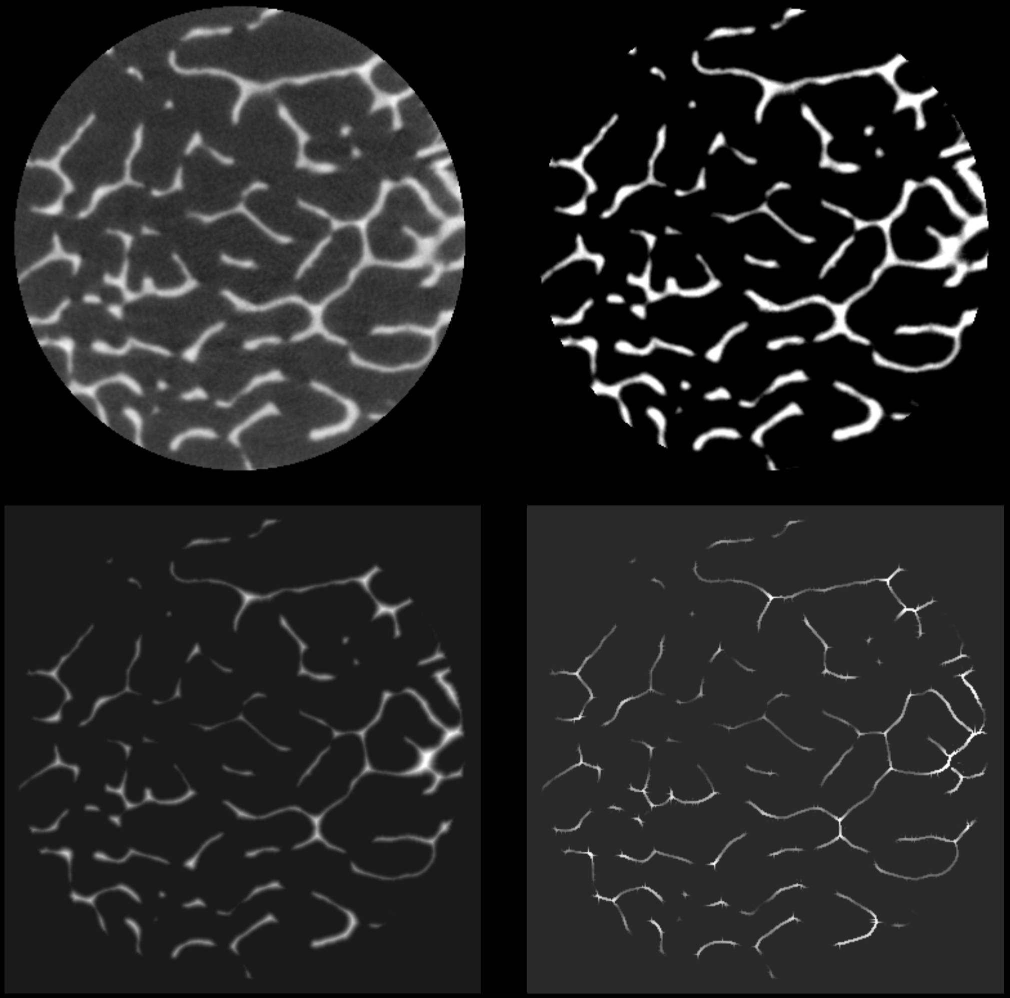

Examples

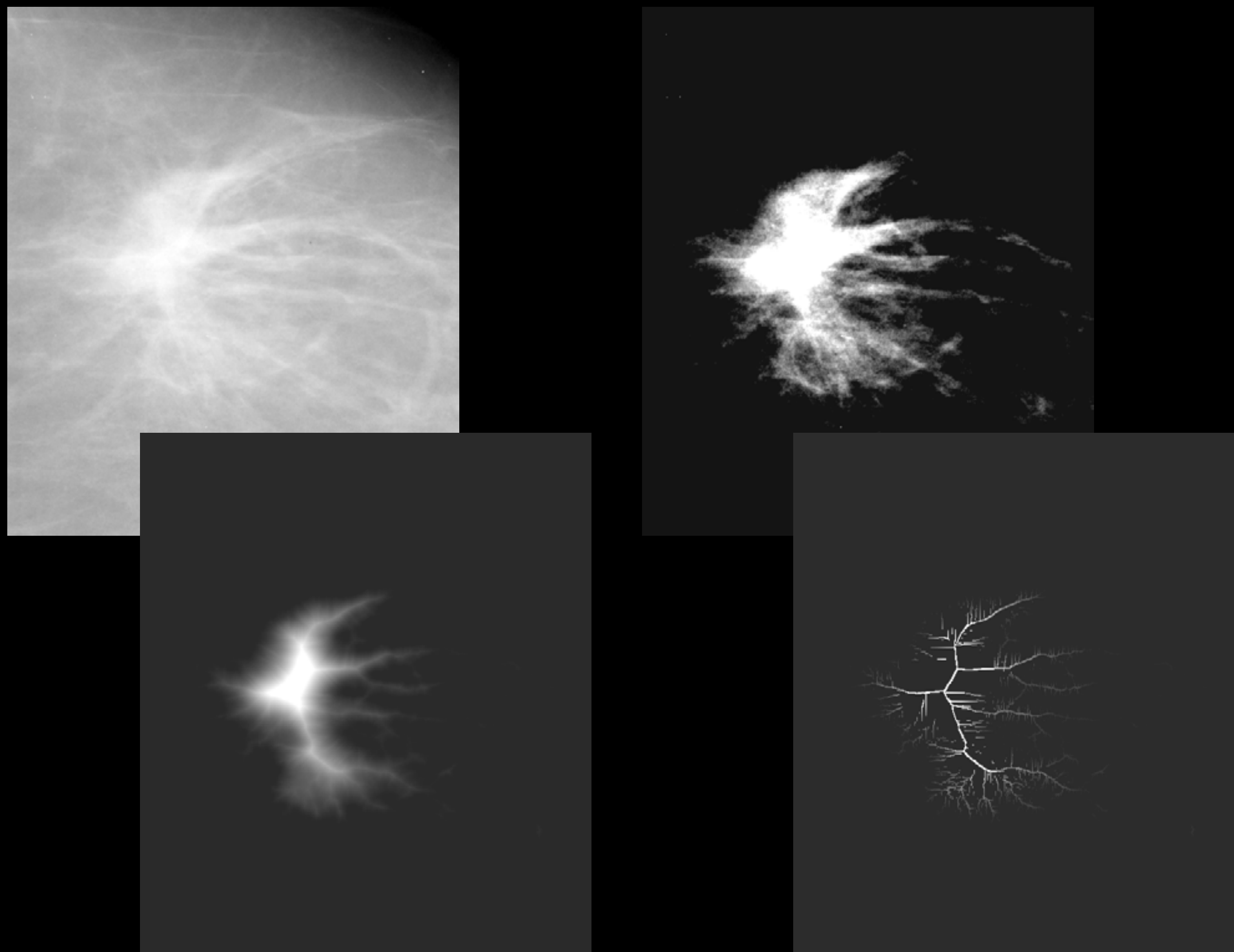

Collision Impact at Quench Voxels

- At a quench voxel, the natural speed of fire-front propagation is interrupted by colliding impulse from opposite fire-fronts
- Collision Impact is defined as the measure of this "degree of colliding impulse"

$$\xi_D(p) = 1 - f_+\left(\max_{q \in N^*(p)} \frac{FDT(q) - FDT(p)}{\frac{1}{2}\left(f_O(p) + f_O(q)\right)|p-q|}\right)$$

- Collision impact determines the significance of individual quench voxels

Filtering Quench Voxels $\Rightarrow$ Axial Voxels

- Too many spurious quench voxels

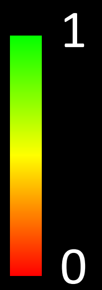

Collision Impact

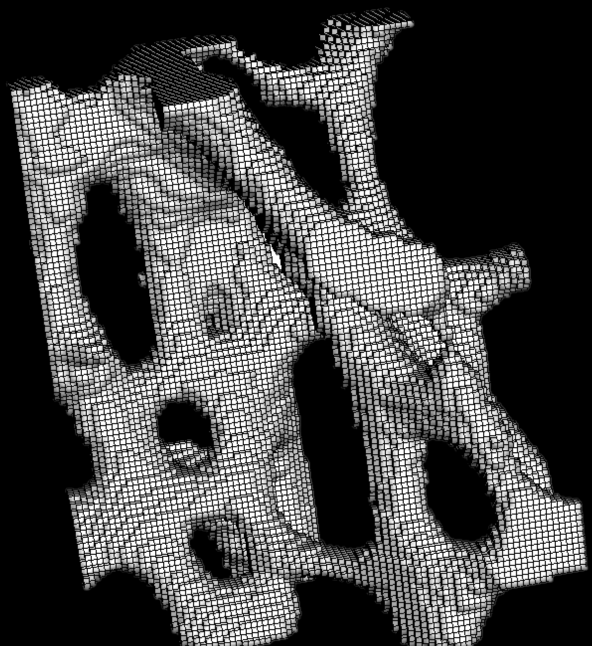

Support of the fuzzy object

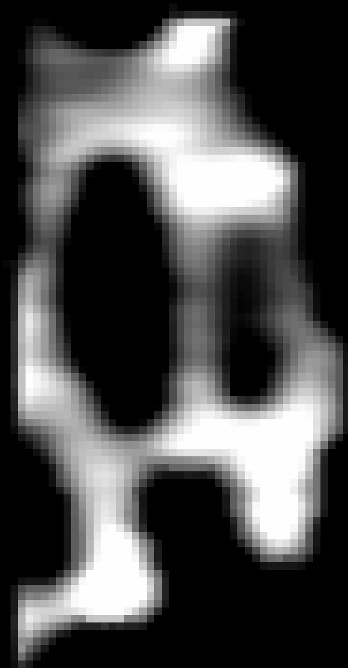

An image slice of the fuzzy object

All quench voxels

Surface and Curve Quench Voxels

- Surface Quench Voxels
  - two opposite fire fronts meet

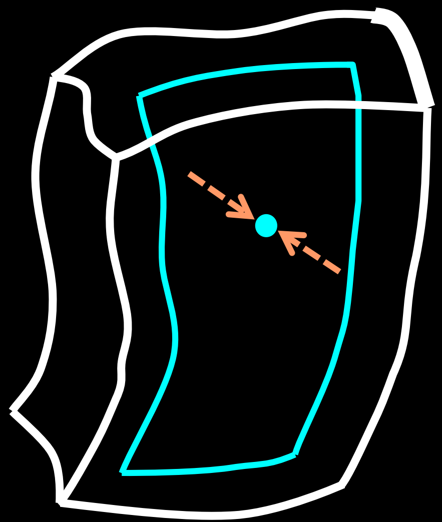

- Curve Quench Voxels
  - fire fronts meet from all directions on a plane

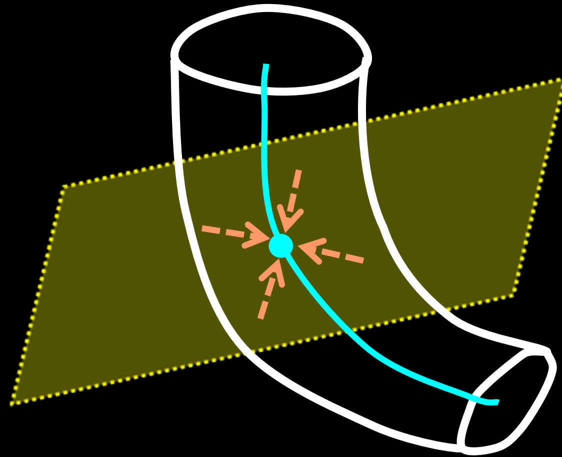

Filtering Quench Voxels

- Define a suitable support mask that fits the geometric type of the quench voxel to consider
- Determine the significance in terms of collision impact over the support mask

Support mask for a surface quench voxel

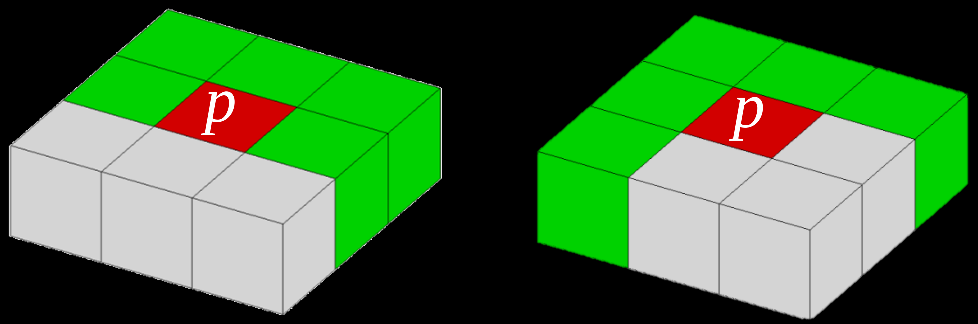

Overall significance

- compute minimum collision impact over the support mask

or

- compute the average collision impact over the support mask

Filtered Axial Voxels

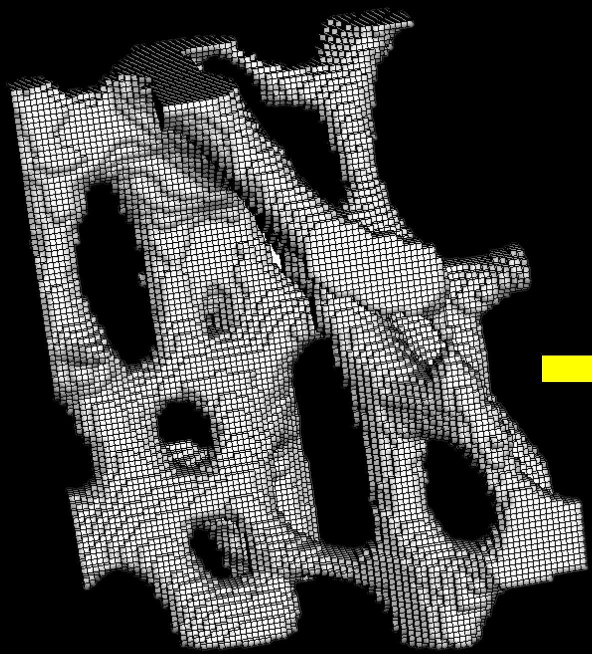

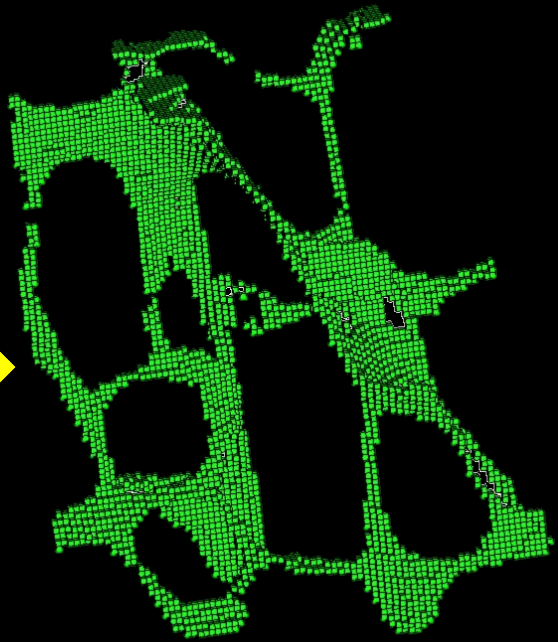

Support of the fuzzy object

All quench voxels

Filtered axial voxels

Skeletal Pruning

- Compute global shape factor of each branch by adding collision impact values of individual voxels and prune spurious branches

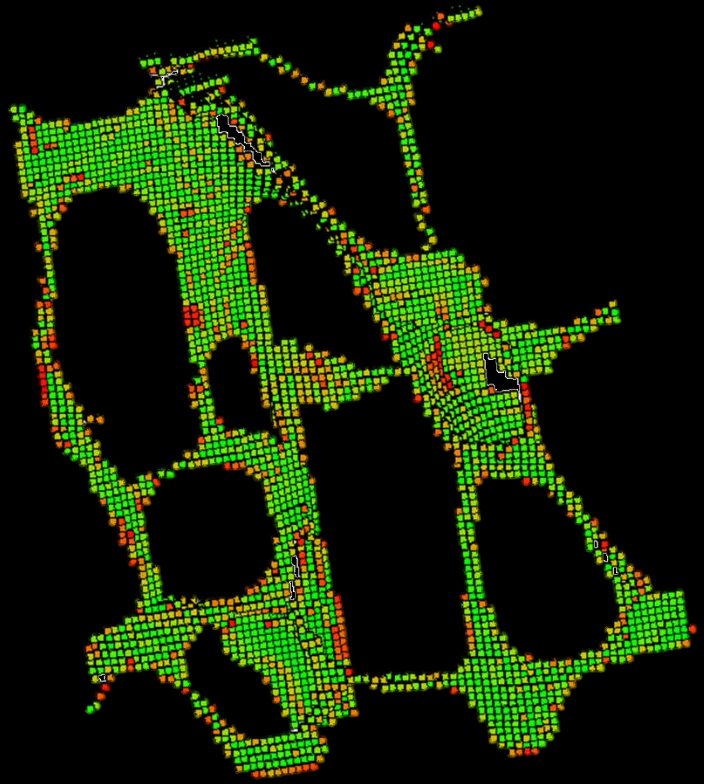

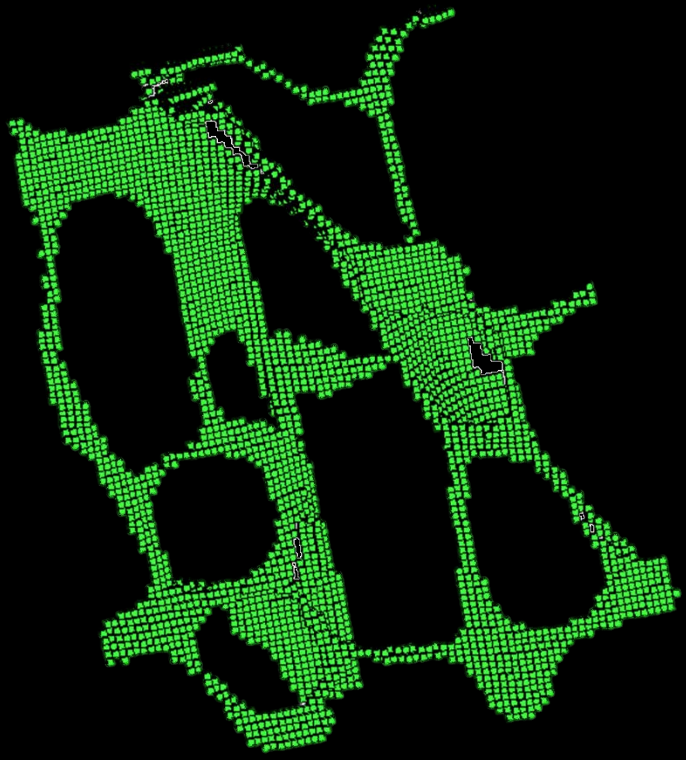

A Few Examples

A Few Examples

Evaluation

- Ground truth: High resolution 3-D binary objects with known skeletons

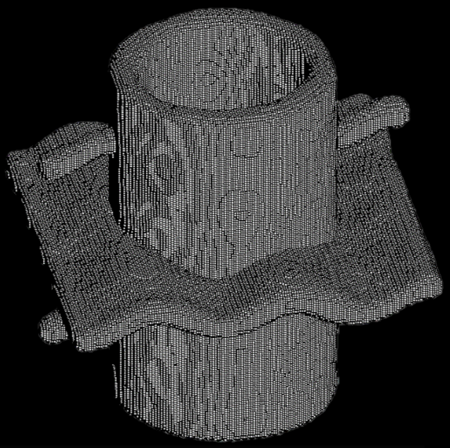

- Test phantoms: Down-sampling binary objects and addition of white Gaussian noise to generate fuzzy objects

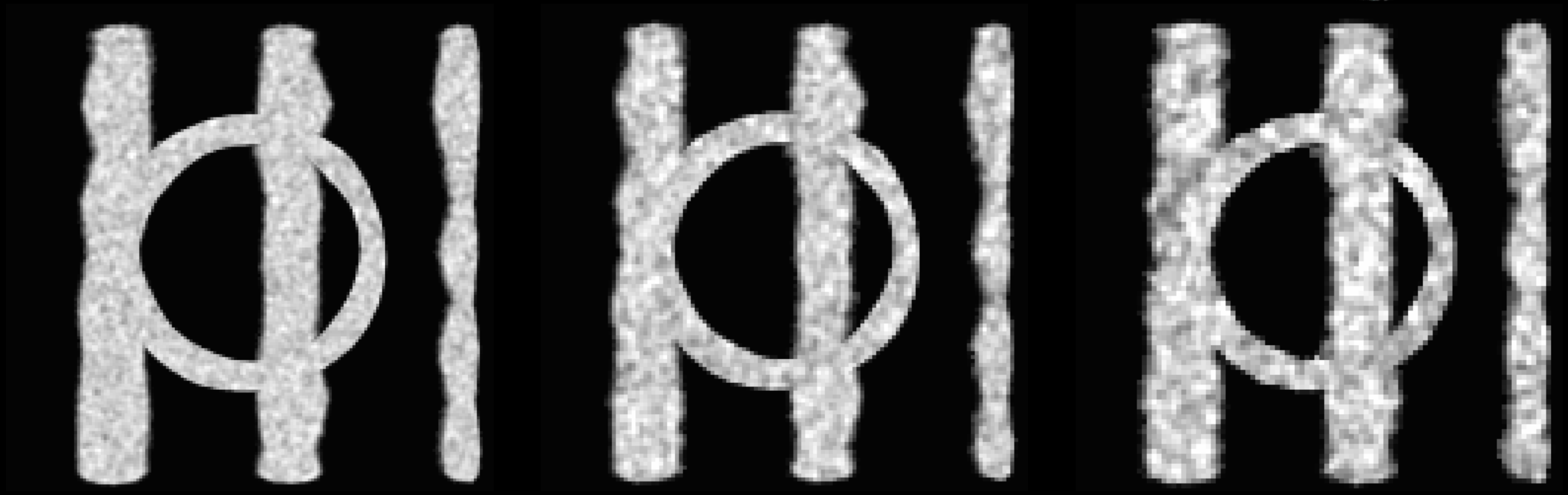

low noise/blur medium noise/blur high noise/blur

Results

- Skeletons at low, medium, and high noise/blur

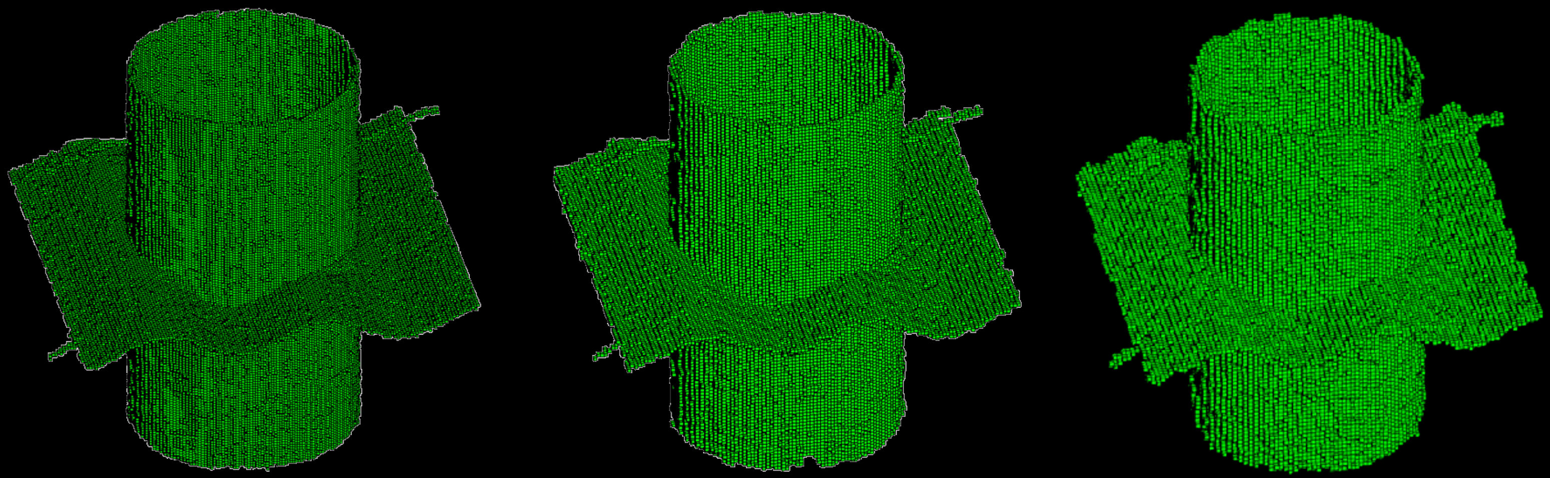

- Fuzzy skeletonization errors in voxel unit

Downsampling	No noise	SNR 24	SNR 12	SNR 6
3×3×3	0.49	0.52	0.54	0.58
4×4×4	0.52	0.53	0.54	0.58
5×5×5	0.57	0.58	0.59	0.60

Outline

- Fuzzy Skeletonization
- Applications of Digital Topology and Geometry in Object Characterization

Bone Morphology & Osteoporosis

- Trabecular bone: network of interconnected plates and rods
- Wolff's law (1892): bone grows/remodels in response to the applied stresses
- Osteoporosis: low bone mineral density and architectural deterioration
- At risk in USA: >40 million
- US health care cost: ~$17B/Y

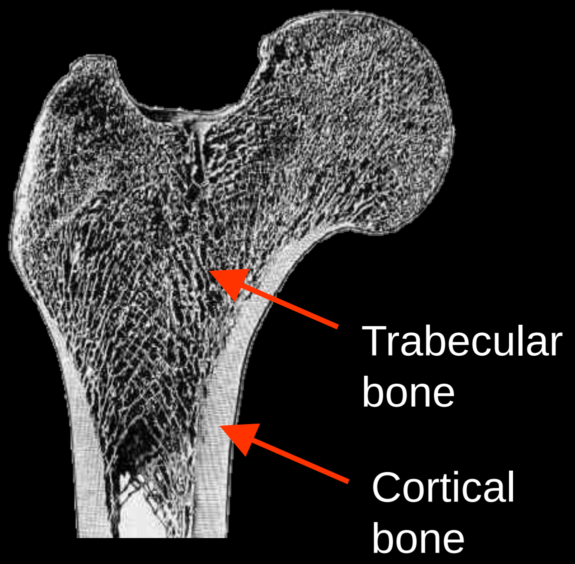

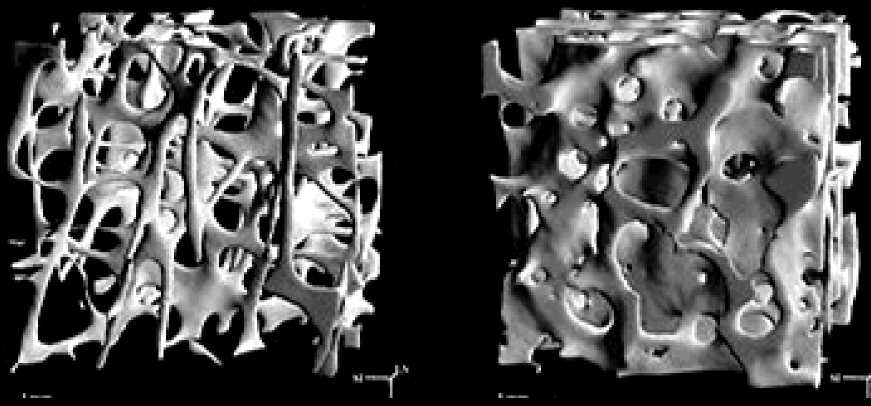

Need improved imaging methods for monitoring bone quality

Bone Mineral Density (BMD) & Architecture

How Predictive is BMD of the Bone's Mechanical Behavior?

- Meta analysis
- N=38 (1985-2000)
- Various parameters of "strength"
- Mean $r^2 = 0.64 \pm 0.17$

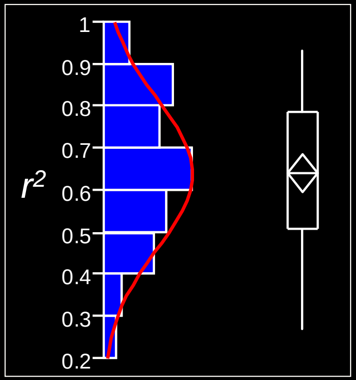

A large number of clinical studies confirm the role of bone architecture to determine bone strength

Quantifying Architecture via Bone Biopsy

- Iliac crest or rib
- Painful, risky, and limited retests
- Not suitable for controls or time-series analysis

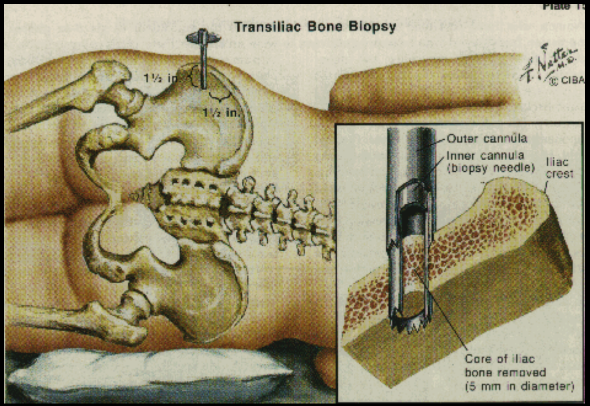

MDCT Offers an Opportunity for Virtual Bone Biopsy

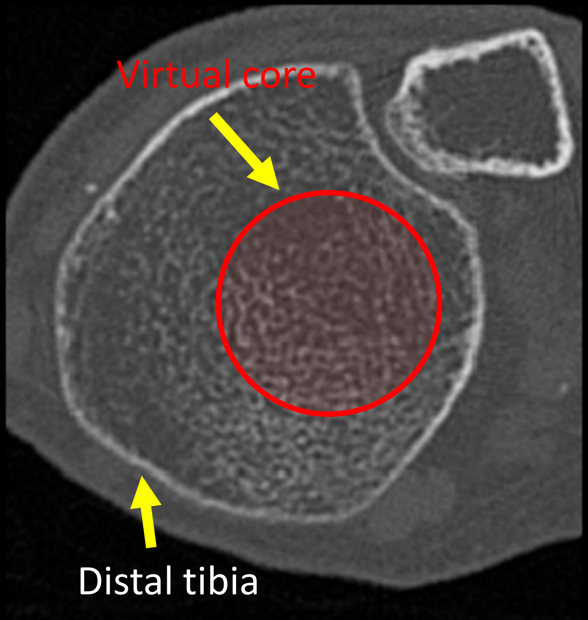

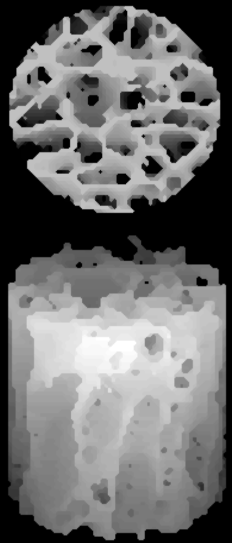

Topology, Scale, Orientation

Challenges

- Reduced resolution
- Limited signal-to-noise ratio

Features

- Analogous to bone biopsy
- Virtual core is isolated from 3D image data sets.
- Core is subjected to analysis

Needs: Improved Morphometric Approaches

Topology of Trabecular Networks

Topological analysis of line skeletonized structure

3D Euler Poincaré Formula

$N^{(3)}$ = objects - tunnels + cavities
= nodes - edges + faces

Connectivity Index = $1-N^{(3)}$

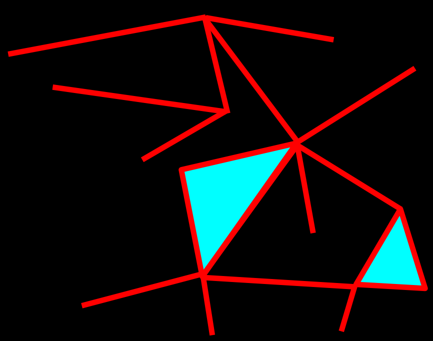

# objects:	1
# tunnels:	1
# cavities:	0
# nodes:	17
# edges:	19
# faces:	2

$N^{(3)} = 0$

Structure-Model Index (SMI)

SMI μ (∂BS/∂r)

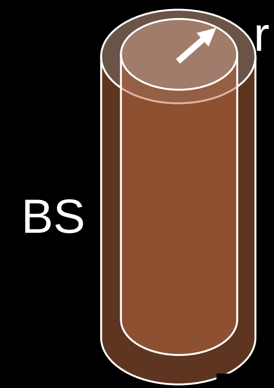

SMI=relative change in surface area upon radial expansion

calcaneus

SMI = 2.3

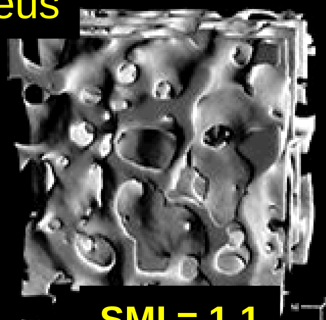

SMI = 1.1

Hildebrand et al, J Bone Miner Res, 1999

Digital Topological Analysis

- Topological class (curve, surface junctions) at any location may be unambiguously determined from the topological numbers (#objects (ξ), #tunnels (η), and #cavities (δ))
- Edge: $\xi = 1; \eta = 0; \delta = 0;$
- Curve Interior: $\xi = 2; \eta = 0; \delta = 0;$
- Surface Interior: $\xi = 1; \eta = 1; \delta = 0$
- Curve-Curve junction: $\xi > 2; \eta = 0; \delta = 0$
- Surface-Curve junction: $\xi > 1; \eta \geq 1; \delta = 0$

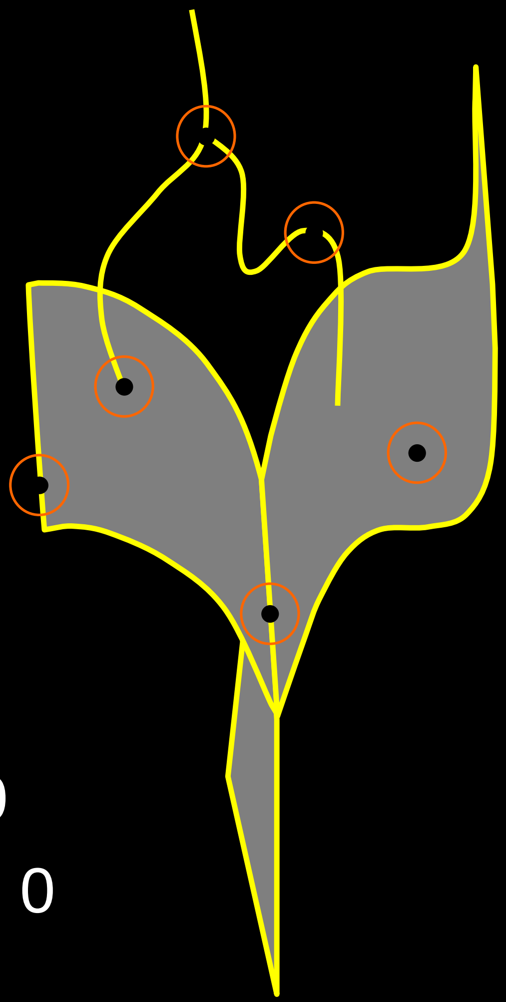

Theory: Saha et al., PR’94, IEEE PAMI’94, CVIU’96, PR’96
Application: Saha, Gomberg & Wehrli, Int J Im Sci Tech’00

Digital Topological Analysis

- Identifies plates/rods and other topological entities
- Able to distinguish between fracture/ non-fracture groups via *in vivo* MRI
- Being used by several leading research groups

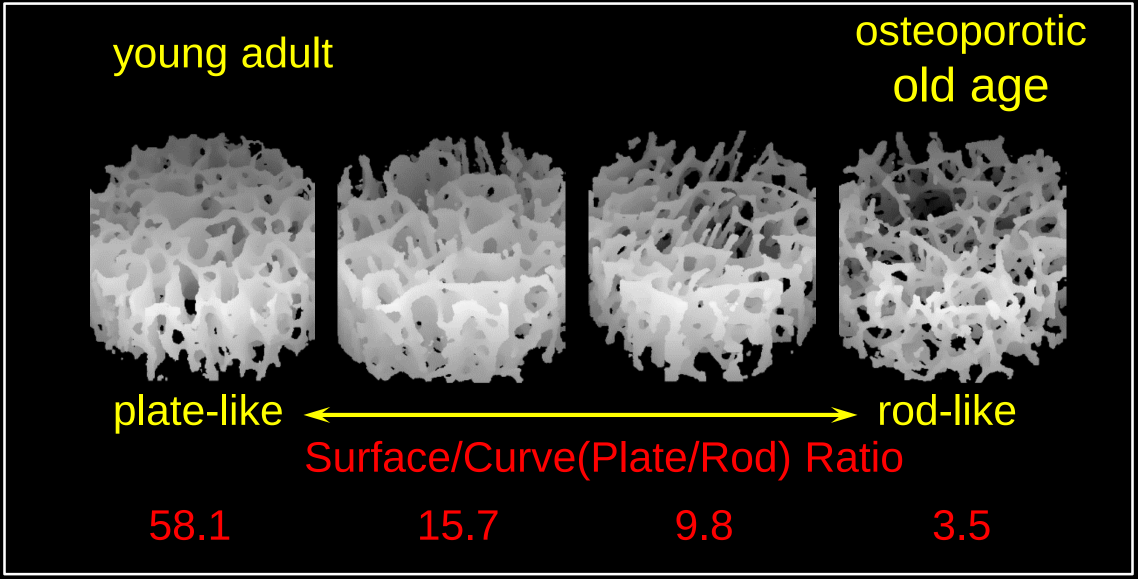

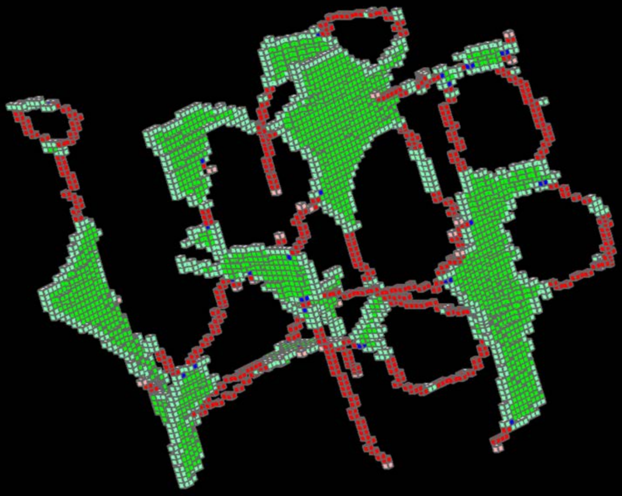

Surface = plate
Rod = curve
Junction

Age and disease-related topological changes

Measures TB thickness/Spacing at *In Vivo* Resolution using Fuzzy Distance Transform

In vivo evidence of Dexamethasone on trabecular bone thickness

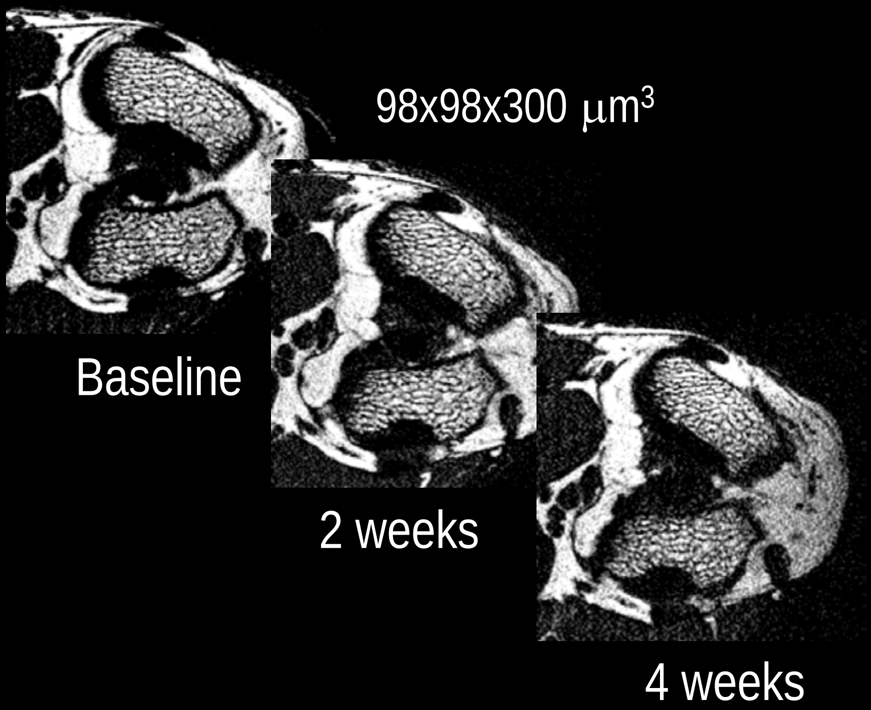

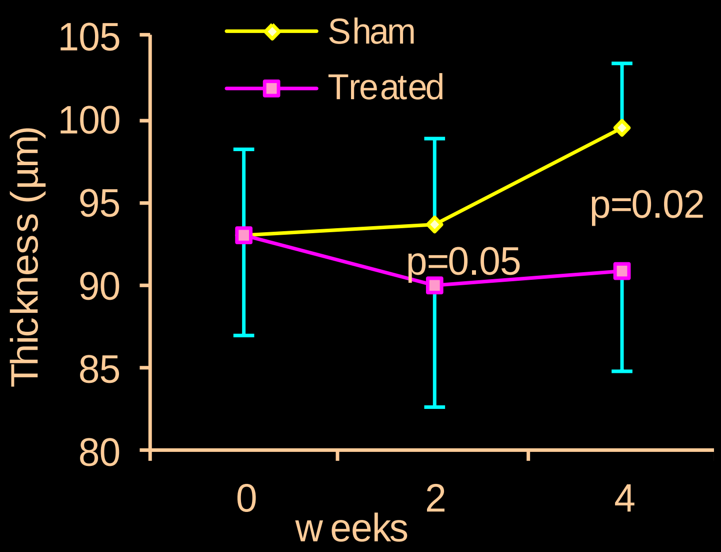

Saha, & Wehrli, IEEE TMI, **23**, 2004

Treatment effect is not visually apparent!

Recent Works: Volumetric Topological Analysis

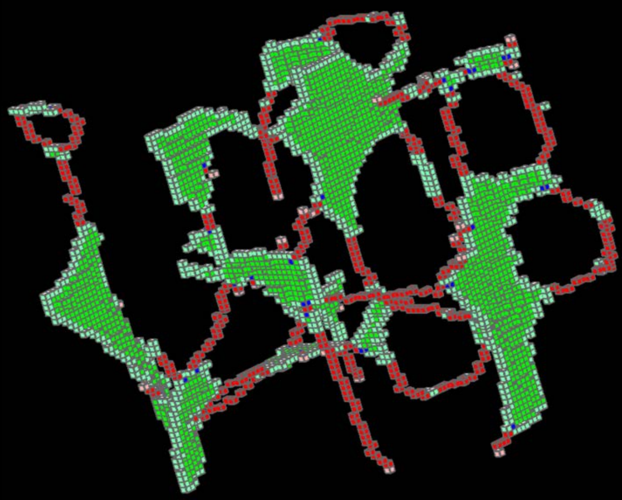

DTA

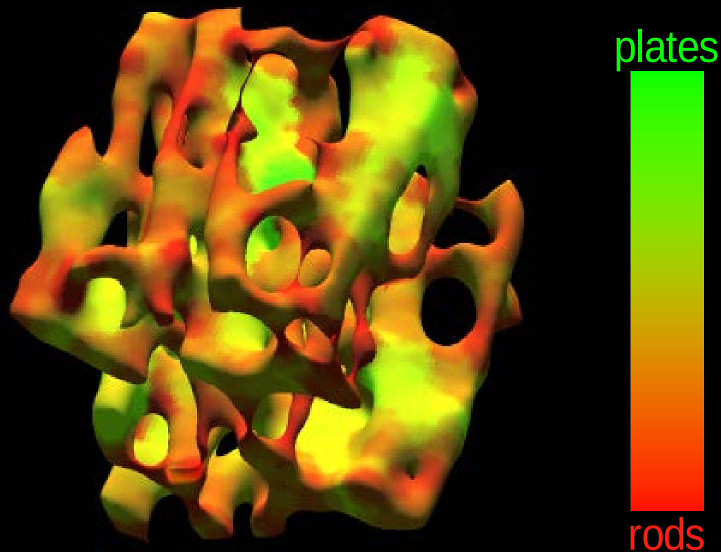

VTA

- Quantify trabecular bone architecture via clinical CT imaging
  - Plateness and rodness on the continuum between perfect plates and perfect rods
  - Local trabecular bone width in the unit of microns

Saha et al. *IEEE Med Imag'10*

How?

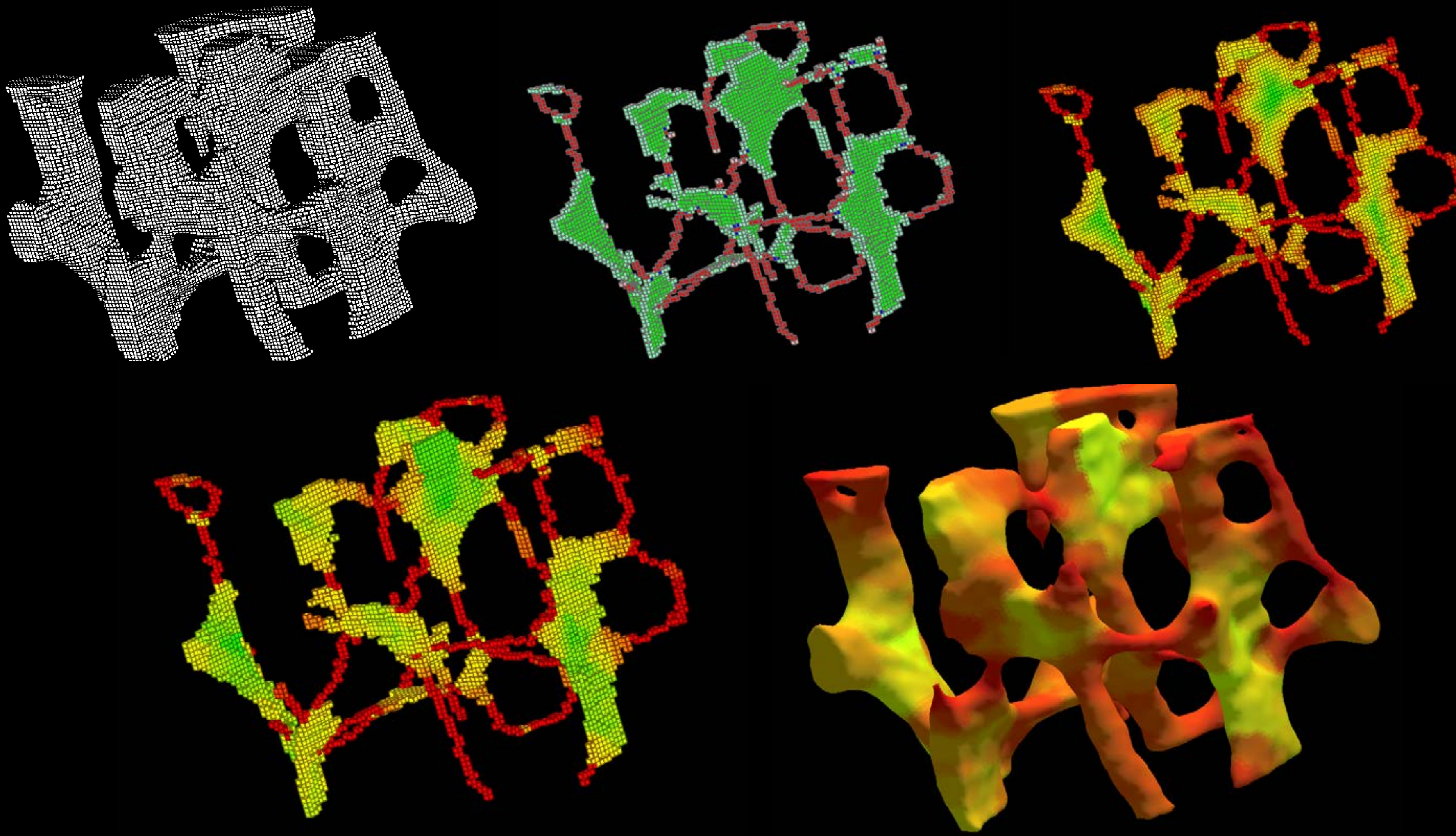

CT Imaging

- 128 slice SOMATOM Definition Siemens Flash scanner
- 120 kV, 200 mAs, pitch: 1.0
- nominal collimation: 16x0.3mm
- scan length: 10 cm
- slice thickness: 300 μm
- total effective dose equivalent:17 mrem ≈ 20 days of environmental radiation

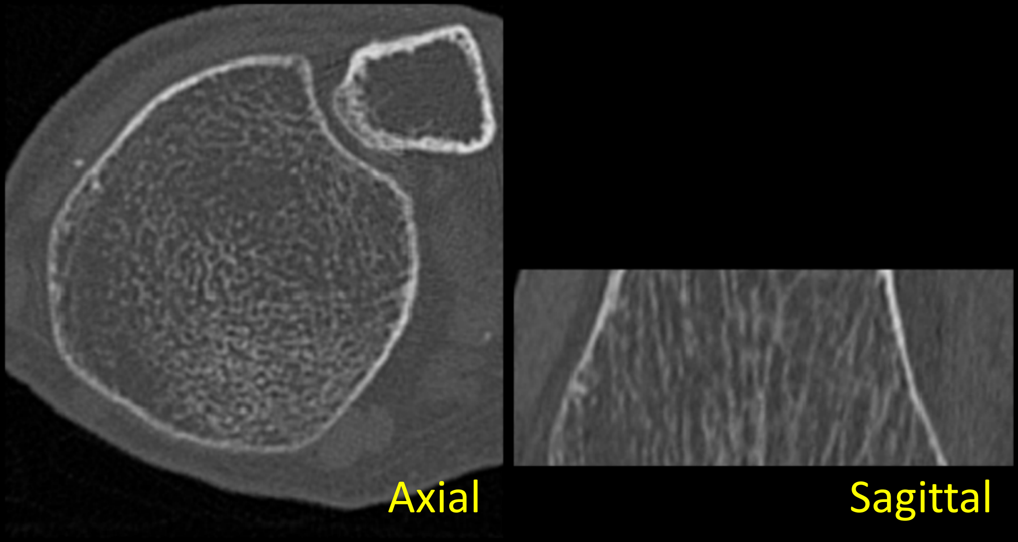

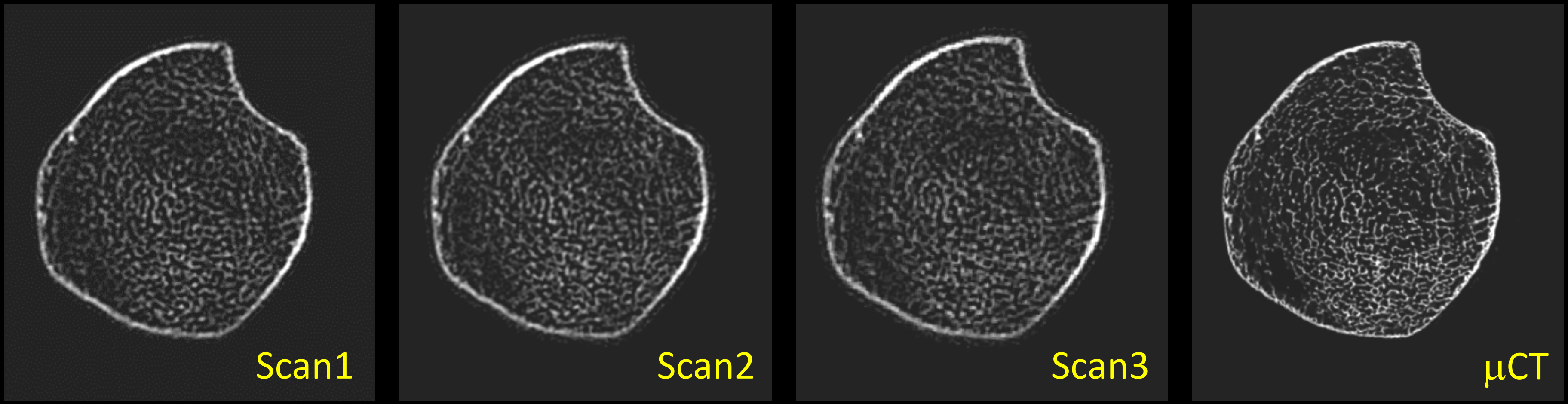

High Intra- and Inter-Modality Reproducibility

Three repeat CT scans

μCT scan

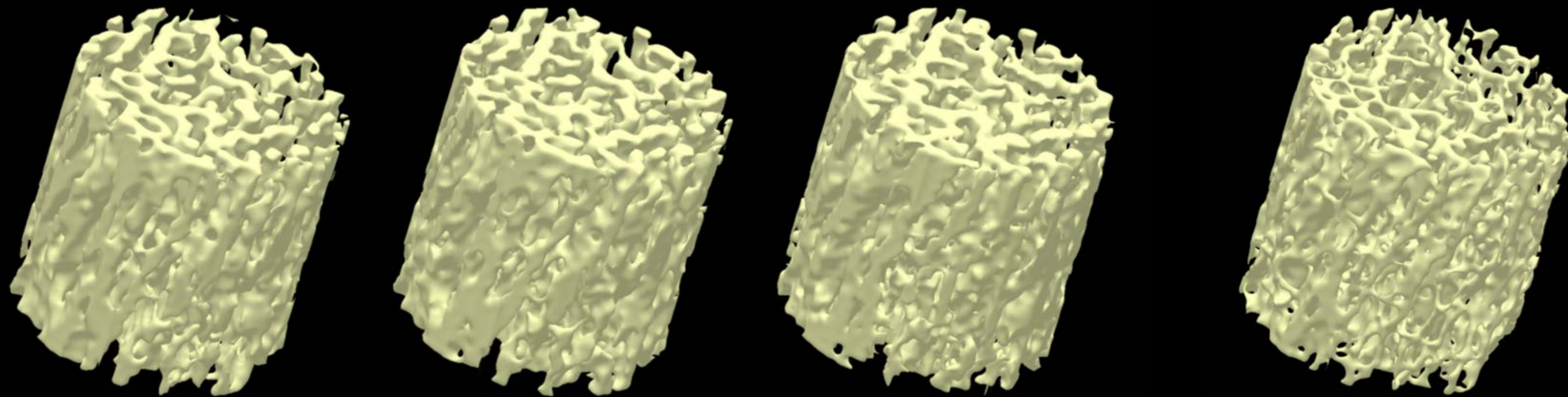

Color-coded results of volumetric topological analysis

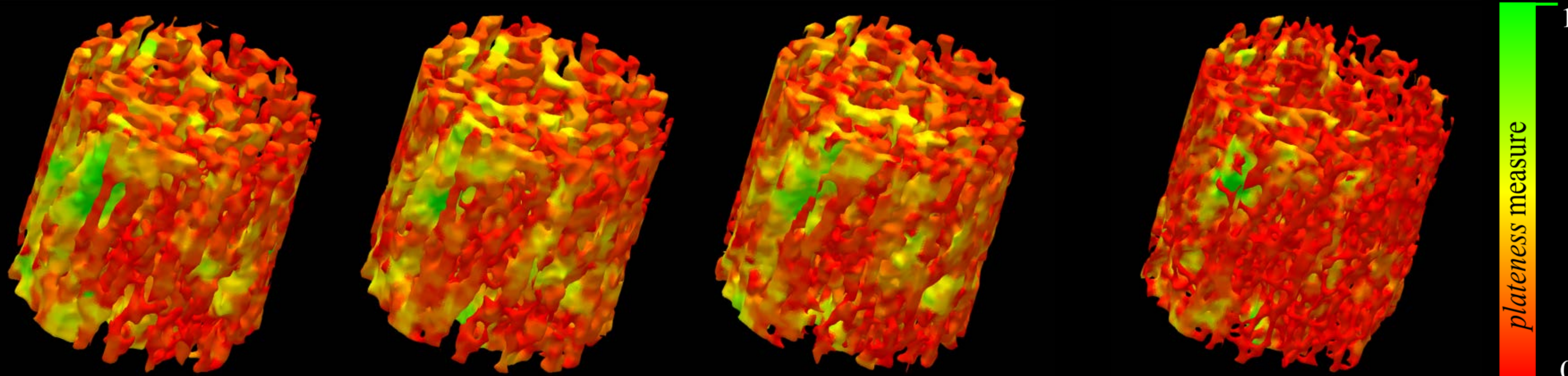

Repeat CT scan ICC: 0.97

Linear correlation CT vs. μCT R^2 =0.93

VTA Measure for TB with Distinctively Different Strengths

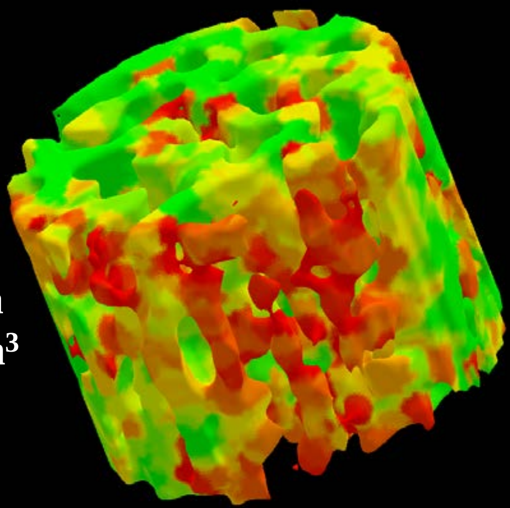

Modulus: 3.3 GPa
BMD: 1.31 gm/cm^3
SW$_{VTA}$: 464 µm
SCR$_{VTA}$: 0.58

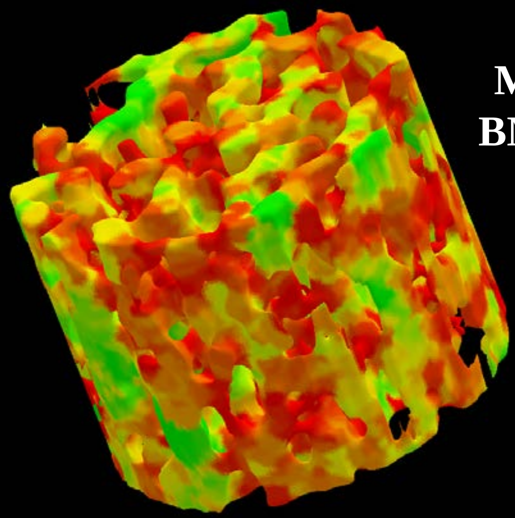

Modulus: 2.2 GPa
BMD: 1.27 gm/cm^3
SW$_{VTA}$: 385 µm
SCR$_{VTA}$: 0.38

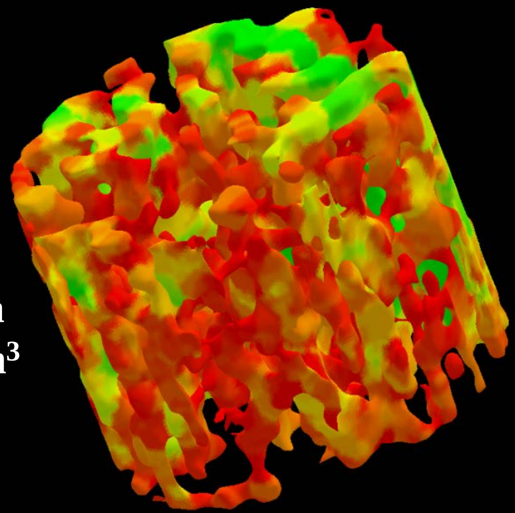

Modulus: 1.5 GPa
BMD: 1.20 gm/cm^3
SW$_{VTA}$: 340 µm
SCR$_{VTA}$: 0.26

8% reduction in BMD reduced bone strength to half and manifest a 50% alteration in micro-architecture

Ability To Predict Mechanical Properties

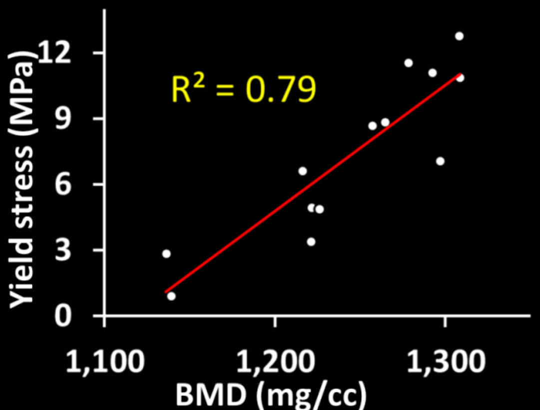

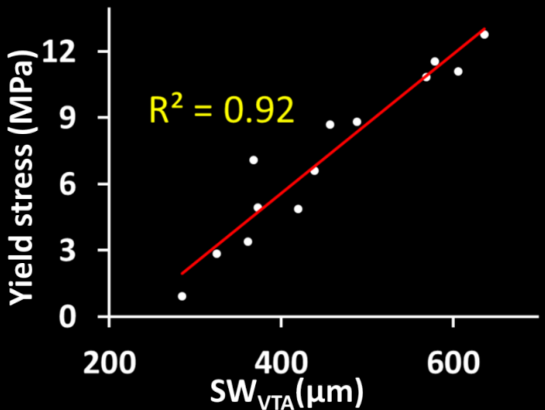

High predictability of experimental biomechanical properties.

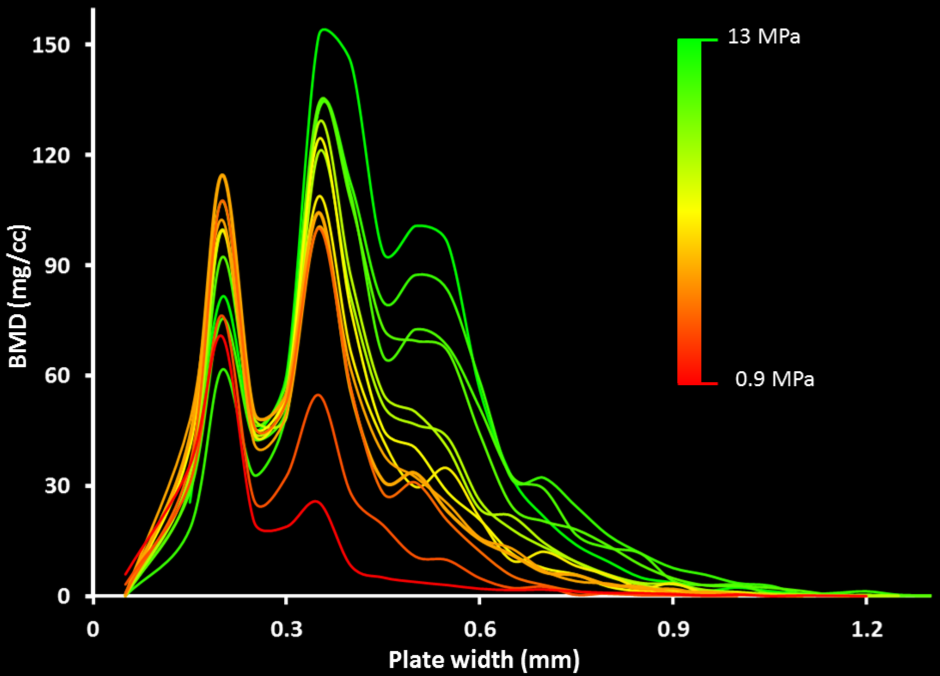

Bone mass distribution at different plate width: a new class of information

Bone Characterization in Different Human Groups

- Age group: 18 to 23 years
- Control Group: Iowa Bone Development Study core of healthy normal (N = 102; 49 males)
- Group 1: Athletes (N = 11; 6 males)
- Group 2: Patients on Selective Serotonin Reuptake Inhibitor (N = 12; 6 males)
- Group 3: Patients with cystic fibrosis (N = 12; 6 males)
- Group 4: Patients with anorexia nervosa (N = 4; 4 females)

Study on Patients with SSRI treatment

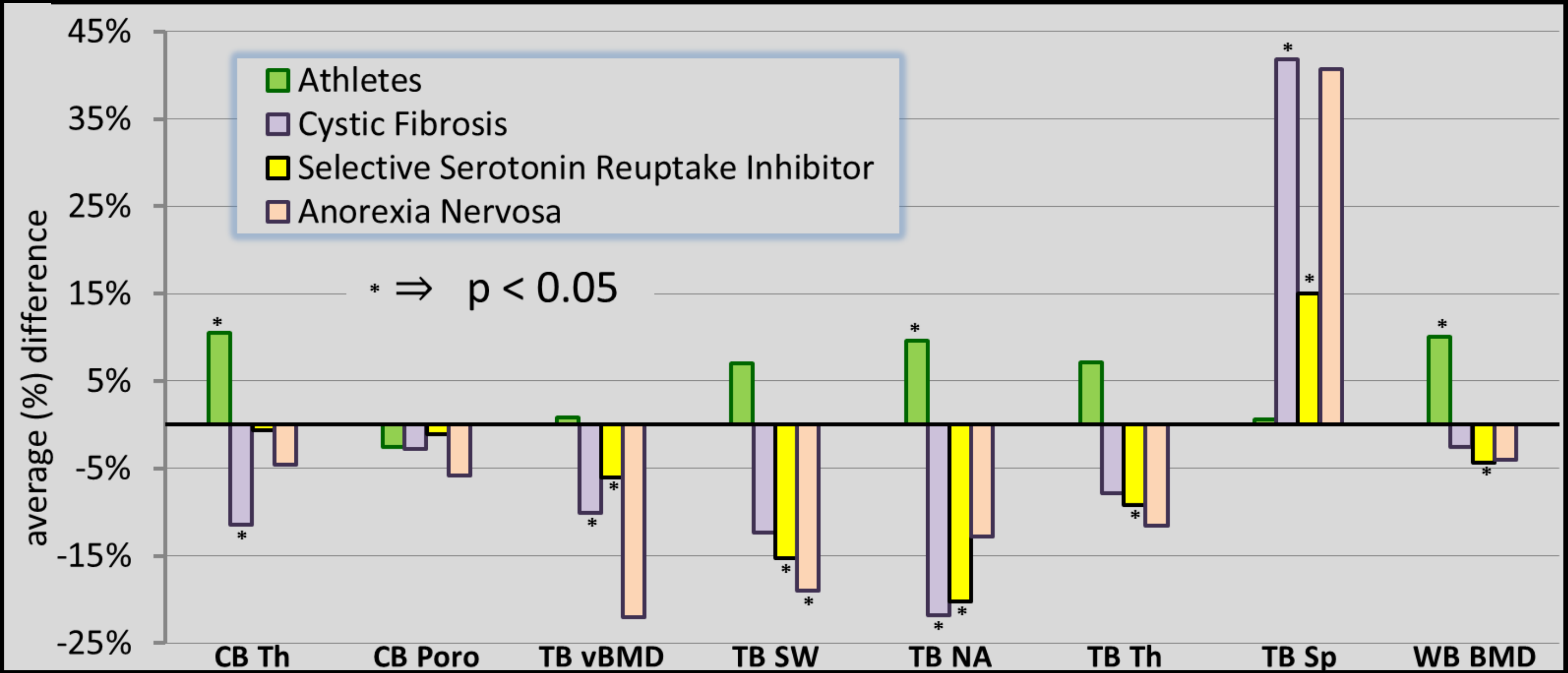

Average differences of bone measures in athlete (N=10), cystic fibrosis (N=11), selective serotonin reuptake inhibitor (N=12), and anorexia nervosa (N=4) groups as compared to age-sex-BMI-similar healthy controls from the Iowa Bone Development Study (N=102). Age-sex-height matching was used for the anorexia nervosa group.

Bone Characterization in Different Human Groups (Qualitative Illustration)

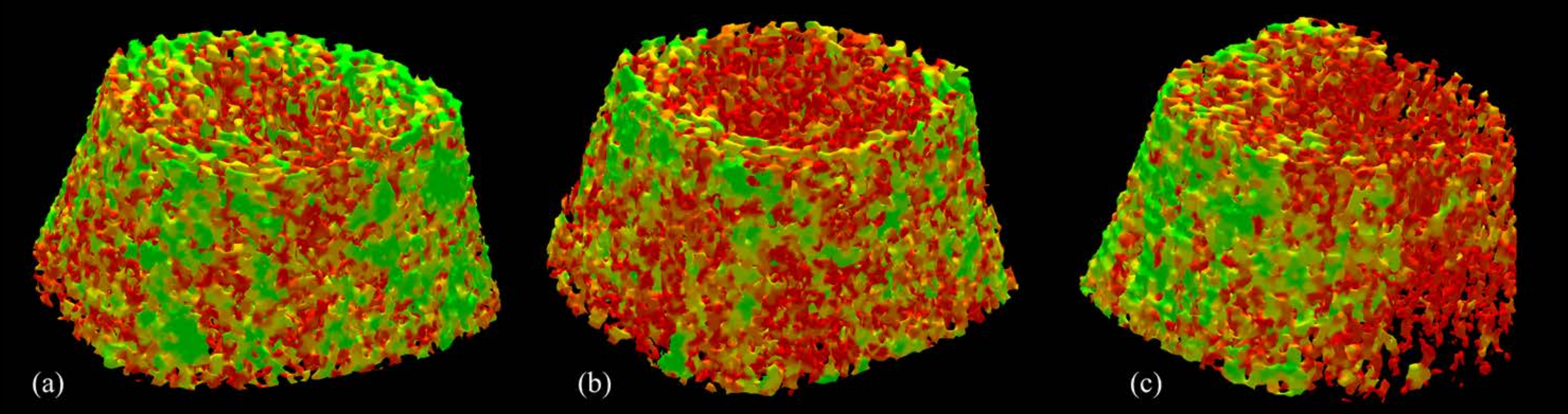

Color-coded illustration of trabecular bone (TB) plate/rod classification for a IBDS female control (a) and an age-similar, sex- and BMI-matched patient on continuous treatment with an SSRI (b), and another age-similar, sex- and BMI-matched patient with confirmed diagnosis of CF (c). The healthy female (a) has more TB plates (green) as compared to the two patient participants. Between the two patients, the CF patient (c) has some signs of heterogeneous bone loss.

Structural Differences in a Fracture vs Non-Fracture Group

- Nineteen subjects with chronic obstructive pulmonary disease
- age: 71.3 ± 8.3 years; BMI: 27.1 ± 4.1
- male: 10; female 9
- 9 subjects with at least one vertebral fracture)

Table 1. Mean±SD of MDCT bone structural measures between fracture () and non-fracture () groups of patients with COPD and the difference (%) between the two groups.

Groups	CB Th(μm)	CB Poro	TB vBMD(mg/cc)	TB PW(μm)	TB Sp(μm)	TB Th(μm)
Fracture	1826±345	0.24±0.09	1270±13	916±119	508±102	121±6
Non-fracture	2061±611	0.17±0.04	1287±16	1027±218	494±155	128±12
Difference	12.1%	32.1%	1.3%	11.5%	2.7%	5.9%

Structural Differences in a Fracture vs Non-Fracture Group

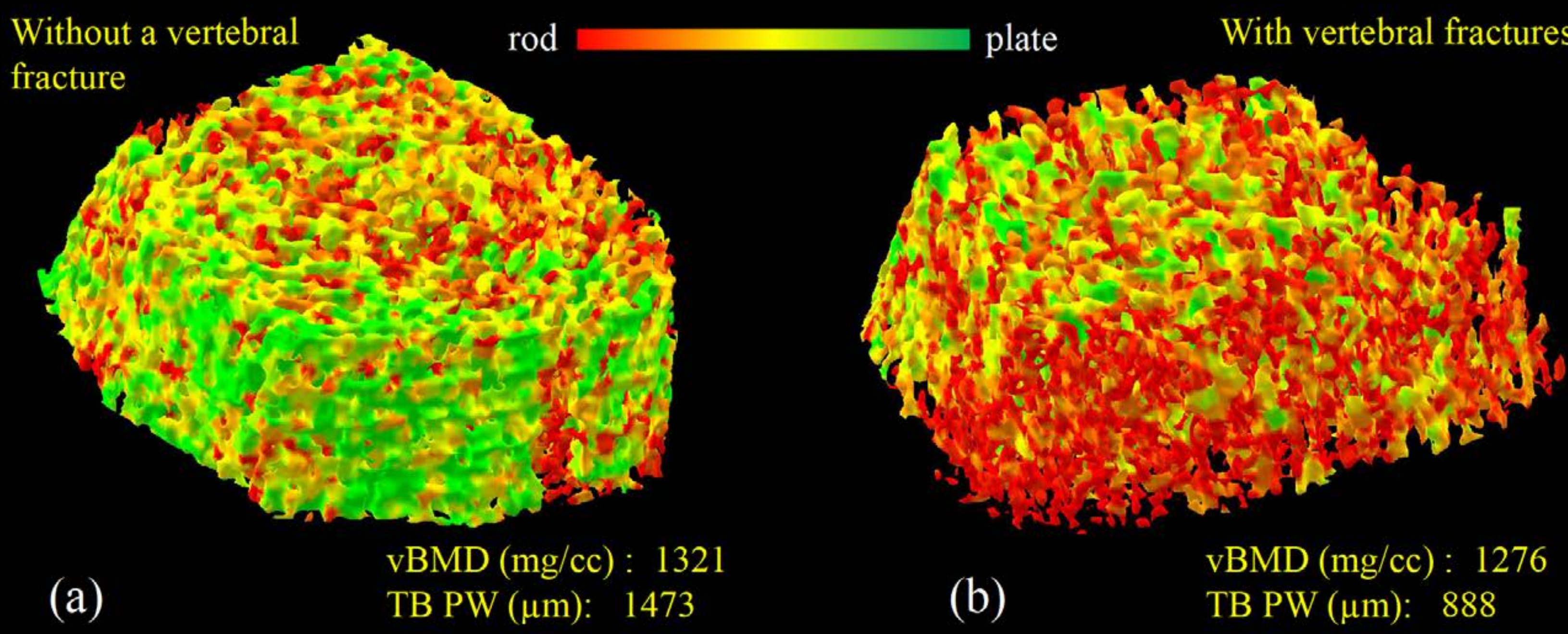

MDCT-derived TB rod / plate classification for a COPD male without (a) and with (b) at least one vertebral fracture. The subject without vertebral fracture has ~50% more TB plates (green) as compared to the subject with at least one vertebral fracture. The difference in TB volumetric BMD between the two subjects is only 3.5%.

Conclusions

- Digital topology and geometry play important roles in medical image processing
  - solves several classical problems of medical imaging
  - expands the scope of target information
  - provides a strong theoretical foundation to a process enhancing its stability, fidelity, and efficiency
- Advanced quantitative characterization of bone micro-architecture are suited for medical imaging research and clinical studies.
- Multi-detector CT is a potential imaging modality for *in vivo* assessment of human trabecular bone micro-architecture

References

[1] JM Abrahams, PK Saha, RW Hurst, PD LeRous, and JK Udupa, "Three dimensional bone-free rendering of the crebral circulation using computed tomographic angiography and fuzzy connectedness," *Neurosurgery*, **51**, 264-269, 2002.

[2] G Chang, SK Pakin, ME Schweitzer, PK Saha, and RR Regatte, "Adaptations in trabecular bone microarchitecture in Olympic athletes determined by 7T MRI," *J Magn Reson Imaging*, **27**, 1089-95, 2008, PubMed Central PMCID: PMCPMC3850284.

[3] G Chang, D Xia, C Chen, G Madelin, SB Abramson, JS Babb, PK Saha, and RR Regatte, "7T MRI detects deterioration in subchondral bone microarchitecture in subjects with mild knee osteoarthritis as compared with healthy controls," *Journal of Magnetic Resonance Imaging*, **41**, 1311-1317, 2015.

[4] C Chen, D Jin, Y Liu, FW Wehrli, G Chang, PJ Snyder, RR Regatte, and PK Saha, "Trabecular bone characterization on the continuum of plates and rods using in vivo MR imaging and volumetric topological analysis," *Physics in Medicine and Biology*, **61**, N478-N496, 2016.

[5] KC Ciesielski, JK Udupa, PK Saha, and Y Zhuge, "Iterative relative fuzzy connectedness for multiple objects with multiple seeds," *Computer Vision and Image Understanding*, **107**, 160-182, 2007.

[6] KC Ciesielski, R Strand, F Malmberg, and PK Saha, "Efficient algorithm for finding the exact minimum barrier distance," *Computer Vision and Image Understanding*, **123**, 53-64, 2014.

[7] S Dudley-Javoroski, PK Saha, G Liang, C Li, Z Gao, and RK Shields, "High dose compressive loads attenuate bone mineral loss in humans with spinal cord injury," *Osteoporosis International*, **23**, 2335-2346, 2012, PubMed Central PMCID: PMC3374128.

[8] S Dudley-Javoroski, R Amelon, YX Liu, PK Saha, and RK Shields, "High bone density masks architectural deficiencies in an individual with spinal cord injury," *Journal of Spinal Cord Medicine*, **37**, 349-354, 2014, PubMed Central PMCID: PMC4064585.

References .....*Continued*

[9] S Dudley-Javoroski, MA Petrie, CL McHenry, RE Amelon, PK Saha, and RK Shields, "Bone architecture adaptations after spinal cord injury: impact of long-term vibration of a constrained lower limb," *Osteoporosis International*, 1-12, 2015.

[10] S Dudley-Javoroski, M Petrie, C McHenry, R Amelon, P Saha, and R Shields, "Bone architecture adaptations after spinal cord injury: impact of long-term vibration of a constrained lower limb," *Osteoporosis International*, **27**, 1149-1160, 2016.

[11] Z Gao, R Grout, C Holtze, EA Hoffman, and PK Saha, "A new paradigm of interactive artery/vein separation in non-contrast pulmonary CT imaging using multi-scale topo-morphologic opening," *IEEE Trans Biomed Eng*, **59**, 3016-3027, 2012.

[12] BR Gomberg, PK Saha, HK Song, SN Hwang, and FW Wehrli, "Topological analysis of trabecular bone MR images," *IEEE Transactions on Medical Imaging*, **19**, 166-174, 2000.

[13] BR Gomberg, FW Wehrli, B Vasilic, RH Weening, PK Saha, HK Song, and AC Wright, "Reproducibility and error sources of micro-MRI-based trabecular bone structural parameters of the distal radius and tibia," *Bone*, **35**, 266-76, 2004.

[14] BR Gomberg, PK Saha, and FW Wehrli, "Method for cortical bone structural analysis from magnetic resonance images," *Academic Radiology*, **12**, 1320-1332, 2005.

[15] LM Griffin, S Honig, C Chen, PK Saha, R Regatte, and G Chang, "7T MRI of distal radius trabecular bone microarchitecture: How trabecular bone quality varies depending on distance from end-of-bone," *Journal of Magnetic Resonance Imaging*, 2016.

[16] A Hotca, CS Rajapakse, C Cheng, S Honig, K Egol, RR Regatte, PK Saha, and G Chang, "In vivo measurement reproducibility of femoral neck microarchitectural parameters derived from 3T MR images," *Journal of Magnetic Resonance Imaging*, 2015.

References .....*Continued*

[17] KS Iyer, JD Newell Jr, D Jin, MK Fuld, PK Saha, S Hansdottir, and EA Hoffman, "Quantitative dual-energy computed tomography supports a vascular etiology of smoking-induced inflammatory lung disease," *American journal of respiratory and critical care medicine*, **193**, 652-661, 2016.

[18] D Jin and PK Saha, "A new fuzzy skeletonization algorithm and its applications to medical imaging," Proc. of *17th Int Conf Imag Anal Proc (ICIAP)*, **LNCS 8156**, 662-671, Naples, Italy, September 11-13 2013.

[19] D Jin, Y Liu, and PK Saha, "Application of fuzzy skeletonization to quantitative assess of trabecular bone micro-architecture," Proc. of *35th International Conference of the IEEE Engineering in Medicine and Biology Society,* Osaka, Japan, July 3-7 2013.

[20] D Jin, KS Iyer, EA Hoffman, and PK Saha, "A New Approach of Arc Skeletonization for Tree-Like Objects Using Minimum Cost Path," Proc. of *22nd International Conference on Pattern Recognition*, 942-947, Stockholm, Sweden, 24-28 August 2014.

[21] D Jin, KS Iyer, EA Hoffman, and PK Saha, "Automated assessment of pulmonary arterial morphology in multi-row detector CT imaging using correspondence with anatomic airway branches," Proc. of *International Symposium on Visual Computing (ISVC)*, **LNCS 8887**, 521-530, Las Vegas, NV, December 8-10 2014.

[22] D Jin, C Chen, and PK Saha, "Filtering non-significant quench points using collision impact in grassfire propagation," Proc. of *18th Int Conf Imag Anal Proc (ICIAP)*, **9279** 432-443, Genoa, Italy, September 9-11 2015.

[23] D Jin, KS Iyer, C Chen, EA Hoffman, and PK Saha, "A robust and efficient curve skeletonization algorithm for tree-like objects using minimum cost paths," *Pattern Recognition Letters*, **76**, 32-40, 2016.

[24] CE Jones, RL Wolf, JA Detre, B Das, PK Saha, J Wang, Y Zhang, HK Song, AC Wright, ER Mohler, RM Fairman, EL Zager, OC Velazquez, MA Golden, JP Carpenter, and FW Wehrli, "Structural MRI of carotid artery atherosclerotic lesion burden and characterization of hemispheric cerebral blood flow before and after carotid endarterectomy," *NMR in Biomedicine*, **19**, 198-208, 2006.

References .....*Continued*

[25] TY Kong, PK Saha, and A Rosenfeld, "Strongly normal sets of tiles in n-dimensions," *Pattern Recognition*, **40**, 530-543, 2007.

[26] GA Ladinsky, B Vasilic, A Popescu, M Wald, B Zemel, PJ Snyder, L Loh, HK Song, PK Saha, AC Wright, and FW Wehrli, "Trabecular structure correlates of vertebral deformity by micro-MRI," Proc. of *Bone quality: What is it and Can We Measure it?*, 27, Bethesda, 2005.

[27] GA Ladinsky, B Vasilic, A Popescu, M Wald, B Zemel, PJ Snyder, L Loh, HK Song, PK Saha, AC Wright, and FW Wehrli, "Degree of Vertebral Deformities is Associated with Topology of Trabecular Network Measured Noninvasively at Radius and Tibia Surrogate Sites," Proc. of *ASBMR, 27th Annual Meeting*, **in press**, S383, Nashville, 2005.

[28] GA Ladinsky, B Vasilic , AM Popescu, B Zemel, AC Wright, HK Song, PK Saha, H Peachy, PK Snyder, and FW Wehrli, "MRI Based Virtual Bone Biopsy Detects Large One-Year Changes in Trabecular Bone Architecture of Early Postmenopausal Women," Proc. of *ASBMR, 27th Annual Meeting*, S15, Nashville, 2005.

[29] GA Ladinsky, B Vasilic, AM Popescu, M Wald, BS Zemel, PJ Snyder, L Loh, HK Song, PK Saha, AC Wright, and FW Wehrli, "Trabecular structure quantified with the MRI-based virtual bone biopsy in postmenopausal women contributes to vertebral deformity burden independent of areal vertebral BMD," *J Bone Miner Res*, **23**, 64-74, 2008, PubMed Central PMCID: PMC2663589.

[30] SC Lam, MJ Wald, CS Rajapakse, Y Liu, PK Saha, and FW Wehrli, "Performance of the MRI-based virtual bone biopsy in the distal radius: serial reproducibility and reliability of structural and mechanical parameters in women representative of osteoporosis study populations," *Bone*, **49**, 895-903, 2011, PubMed Central PMCID: PMC3167016.

[31] T Lei, JK Udupa, PK Saha, and D Odhner, "Artery-vein separation via MRA - an image processing approach," *IEEE Transactions on Medical Imaging*, **20**, 689-703, 2001.

References .....*Continued*

[32] T Lei, JK Udupa, PK Saha, D Odhner, R Baum, ST Tadikonda, and EK Yucel, "3D MRA visualization and Artery-Vein Separation using blood-pool contrast agent MS-325," *Academic Radiology*, **9**, S127-S133, 2002.

[33] C Li, D Jin, C Chen, EM Letuchy, KF Janz, TL Burns, JC Torner, SM Levy, and PK Saha, "Automated cortical bone segmentation for multirow-detector CT imaging with validation and application to human studies," *Med Phys*, **42**, 4553-65, 2015, PubMed Central PMCID: PMC4499051.

[34] XS Liu, P Sajda, PK Saha, FW Wehrli, and XE Guo, "Quantification of the roles of trabecular microarchitecture and trabecular type in determining the elastic modulus of human trabecular bone," *J Bone Miner Res*, **21**, 1608-1617, 2006.

[35] XS Liu, P Sajda, PK Saha, FW Wehrli, G Bevill, TM Keaveny, and XE Guo, "Complete volumetric decomposition of individual trabecular plates and rods and its morphological correlations with anisotropic elastic moduli in human trabecular bone," *J Bone Miner Res*, **23**, 223-35, 2008, PubMed Central PMCID: PMC2665696.

[36] Y Liu, PK Saha, and Z Xu, "Quantitative characterization of trabecular bone micro-architecture using tensor scale and multi-detector CT imaging," Proc. of *Med Image Comput Comput Assist Interv*, **15**, 124-131, 2012.

[37] Y Liu, G Liang, and PK Saha, "A new multi-object image thresholding method based on correlation between object class uncertainty and intensity gradient," *Med Phys*, **39**, 514-32, 2012, PubMed Central PMCID: PMC3266827.

[38] Y Liu, D Jin, C Li, KF Janz, TL Burns, JC Torner, SM Levy, and PK Saha, "A robust algorithm for thickness computation at low resolution and its application to in vivo trabecular bone CT imaging," *IEEE Transactions on Biomedical Engineering*, **61**, 2057-2069, 2014, PubMed Central PMCID: PMCNIHMSID696943.

[39] L Nyúl, JK Udupa, and PK Saha, "Incorporating a measure of local scale in voxel-based 3D image registration," *IEEE Transactions on Medical Imaging*, **22**, 228-237, 2003.

[40] PK Saha, B Chanda, and DD Majumder, "Principles and algorithms for 2-D and 3-D shrinking," Indian Statistical Institute, Calcutta, India, TR/KBCS/2/91, 1991.

References .....*Continued*

[41] PK Saha and BB Chaudhuri, "Simple point computation and 3-D thinning with parallel implementation," Indian Statistical Institute, Calcutta, India, TR/KBCS/1/93, 1993.

[42] PK Saha and BB Chaudhuri, "Detection of 3-D simple points for topology preserving transformations with application to thinning," *IEEE Transactions on Pattern Analysis and Machine Intelligence*, **16**, 1028-1032, 1994.

[43] PK Saha, BB Chaudhuri, B Chanda, and DD Majumder, "Topology preservation in 3D digital space," *Pattern Recognition*, **27**, 295-300, 1994.

[44] PK Saha and BB Chaudhuri, "3D digital topology under binary transformation with applications," *Computer Vision and Image Understanding*, **63**, 418-429, 1996.

[45] PK Saha, BB Chaudhuri, and DD Majumder, "A new shape preserving parallel thinning algorithm for 3D digital images," *Pattern Recognition*, **30**, 1939-1955, 1997.

[46] PK Saha, DD Majumder, and A Rosenfeld, "Local topological parameters in a tetrahedral representation," *Graphical Models Image Processing*, **60**, 423-436, 1998.

[47] PK Saha and A Rosenfeld, "Strongly normal sets of convex polygons or polyhedra," *Pattern Recognition Letters*, **19**, 1119-1124, 1998.

[48] PK Saha, BR Gomberg, and FW Wehrli, "Three-dimensional digital topological characterization of cancellous bone architecture," *International Journal of Imaging Systems and Technology*, **11**, 81-90, 2000.

[49] PK Saha and JK Udupa, "Iterative relative fuzzy connectedness and object definition: theory, algorithms, and applications in image segmentation," Proc. of *IEEE Workshop on Mathematical Methods in Biomedical Image Analysis*, Hilton Head, South Carolina, 2000.

[50] PK Saha, JK Udupa, and D Odhner, "Scale-based fuzzy connected image segmentation: theory, algorithms, and validation," *Computer Vision and Image Understanding*, **77**, 145-174, 2000.

References .....*Continued*

[51] PK Saha and A Rosenfeld, "The digital topology of sets of convex voxels," *Graphical Models Image Processing*, **62**, 343-352, 2000.

[52] PK Saha and A Rosenfeld, "Determining simplicity and computing topological change in strongly normal partial tilings of R^2 or R^3," *Pattern Recognition*, **33**, 105-118, 2000.

[53] PK Saha and JK Udupa, "Relative fuzzy connectedness among multiple objects: theory, algorithms, and applications in image segmentation," *Computer Vision and Image Understanding*, **82**, 42-56, 2001.

[54] PK Saha and JK Udupa, "Fuzzy connected object delineation: axiomatic path strength definition and the case of multiple seeds," *Computer Vision and Image Understanding*, **83**, 275-295, 2001.

[55] PK Saha and JK Udupa, "Scale based image filtering preserving boundary sharpness and fine structures," *IEEE Transactions on Medical Imaging*, **20**, 1140-1155, 2001.

[56] PK Saha and A Rosenfeld, "Local and global topology preservation in locally finite sets of tiles," *Information Sciences*, **137**, 303-311, 2001.

[57] PK Saha and JK Udupa, "Optimum threshold selection using class uncertainty and region homogeneity," *IEEE Transactions on Pattern Analysis and Machine Intelligence*, **23**, 689-706, 2001.

[58] PK Saha, JK Udupa, EF Conant, DP Chakraborty, and D Sullivan, "Breast tissue glandularity quantification via digitized mammograms," *IEEE Transactions on Medical Imaging*, **20**, 792-803, 2001.

[59] PK Saha, FW Wehrli, and BR Gomberg, "Fuzzy distance transform: theory, algorithms, and applications," *Computer Vision and Image Understanding*, **86**, 171-190, 2002.

[60] PK Saha and FW Wehrli, "Fuzzy distance transform in general digital grids and its applications," Proc. of *7th Joint Conference on Information Sciences*, 201-213, Research Triangular Park, NC, 2003.

[61] PK Saha and FW Wehrli, "Measurement of trabecular bone thickness in the limited resolution regime of in vivo MRI by fuzzy distance transform," *IEEE Trans Med Imaging*, **23**, 53-62, 2004.

References .....*Continued*

[62] PK Saha and FW Wehrli, "A robust method for measuring trabecular bone orientation anisotropy at in vivo resolution using tensor scale," *Pattern Recognition*, **37**, 1935-1944, 2004.

[63] PK Saha, JK Udupa, AX Falcão, BE Hirsch, and S Siegler, "Iso-shaping rigid bodies for estimating their motion from image sequences," *IEEE Transactions on Medical Imaging*, **23**, 63-72, 2004.

[64] PK Saha, "Tensor scale: a local morphometric parameter with applications to computer vision and image processing," *Computer Vision and Image Understanding*, **99**, 384-413, 2005.

[65] PK Saha, B Das, and FW Wehrli, "An object class-uncertainty induced adaptive force and its application to a new hybrid snake," *Pattern Recognition*, **40**, 2656-2671, 2007.

[66] PK Saha, Z Gao, SK Alford, M Sonka, and EA Hoffman, "Topomorphologic separation of fused isointensity objects via multiscale opening: separating arteries and veins in 3-D pulmonary CT," *IEEE Transactions on Medical Imaging*, **29**, 840-851, 2010.

[67] PK Saha, Y Xu, H Duan, A Heiner, and G Liang, "Volumetric topological analysis: a novel approach for trabecular bone classification on the continuum between plates and rods," *IEEE Trans Med Imaging*, **29**, 1821-38, 2010, PubMed Central PMCID: PMC3113685.

[68] PK Saha, G Liang, JM Elkins, A Coimbra, LT Duong, DS Williams, and M Sonka, "A new osteophyte segmentation algorithm using partial shape model and its applications to rabbit femur anterior cruciate ligament transection via micro-CT imaging," *IEEE Transactions on Biomedical Engineering*, **58**, 2212-2227, 2011.

[69] PK Saha, R Strand, and G Borgefors, "Digital Topology and Geometry in Medical Imaging: A Survey," *IEEE Trans Med Imaging*, **34**, 1940-64, 2015.

[70] PK Saha, Y Liu, C Chen, D Jin, EM Letuchy, Z Xu, RE Amelon, TL Burns, JC Torner, SM Levy, and CA Calarge, "Characterization of trabecular bone plate-rod microarchitecture using multirow detector CT and the tensor scale: Algorithms, validation, and applications to pilot human studies," *Med Phys*, **42**, 5410-5425, 2015, PubMed Central PMCID: PMC4545095.

References .....*Continued*

[71] PK Saha, G Borgefors, and G Sanniti di Baja, "A survey on skeletonization algorithms and their applications," *Pattern Recognition Letters*, **76**, 3-12, 2016.

[72] PK Saha, G Borgefors, and G Sanniti di Baja, "Skeletonization and its applications-a review," in *Skeletonization: Theory Methods, and Applications*, P. K. Saha, G. Borgefors, and G. Sanniti di Baja, Eds., Academic Press, 2017.

[73] PK Saha, G Borgefors, and G Sanniti di Baja, *Skeletonization: Theory, Methods, and Applications*, Academic Press, 2017.

[74] PK Saha, D Jin, Y Liu, GE Christensen, and C Chen, "Fuzzy object skeletonization: theory, algorithms, and applications," *IEEE Transactions on Visualization and Computer Graphics*, in press.

[75] N Sladoje, I Nyström, and PK Saha, "Measurements of digitized objects with fuzzy borders in 2D and 3D," *Image and Vision Computing*, **23**, 123-132, 2005.

[76] R Strand, KC Ciesielski, F Malmberg, and PK Saha, "The minimum barrier distance," *Computer Vision and Image Understanding*, **117**, 429-437, 2013.

[77] JK Udupa, PK Saha, and RA Lotufo, "Relative fuzzy connectedness and object definition: theory, algorithms, and applications in image segmentation," *IEEE Transactions on Pattern Analysis and Machine Intelligence*, **24**, 1485-1500, 2002.

[78] JK Udupa and PK Saha, "Fuzzy connectedness and image segmentation," *Proceedings of the IEEE*, **91**, 1649-1669, 2003.

[79] DM Vasilescu, Z Gao, PK Saha, L Yin, G Wang, B Haefeli-Bleuer, M Ochs, ER Weibel, and EA Hoffman, "Assessment of morphometry of pulmonary acini in mouse lungs by nondestructive imaging using multiscale microcomputed tomography," *Proc Natl Acad Sci U S A*, **109**, 17105-10, 2012, PubMed Central PMCID: PMC3479519.

[80] MJ Wald, B Vasilic, PK Saha, and FW Wehrli, "Spatial autocorrelation and mean intercept length analysis of trabecular bone anisotropy applied to in vivo magnetic resonance imaging," *Med Phys*, **34**, 1110-20, 2007.

References .....*Continued*

[81] FW Wehrli, PK Saha, and BR Gomberg, "Digital topological analysis of trabecular bone MR images and prediction of osteoporosis fractures," *U.S. Application filed by the University of Pennsylvania*, **Penn Docket N2493**, 2000.

[82] FW Wehrli, BR Gomberg, PK Saha, HK Song, SN Hwang, and PJ Snyder, "Digital topological analysis of in vivo magnetic resonance microimages of trabecular bone reveals structural implications of osteoporosis," *Journal of Bone Mineral Research*, **16**, 1520-1531, 2001.

[83] FW Wehrli, PK Saha, BR Gomberg, HK Song, PJ Snyder, M Benito, A Wright, and R Weening, "Role of magnetic resonance for assessing structure and function of trabecular bone," *Top Magn Reson Imaging*, **13**, 335-55, 2002.

[84] FW Wehrli, PK Saha, BR Gomberg, and HK Song, "Noninvasive assessment of bone architecture by magnetic resonance micro-imaging-based virtual bone biopsy," *Proceedings of IEEE, Emerging Medical Imaging Technology, (invited paper)*, **91**, 1520-1542, 2003.

[85] FW Wehrli, MB Leonard, PK Saha, and BG Gomberg, "Quantitative high-resolution MRI reveals structural implications of renal osteodystrophy on trabecular and cortical bone," *J Magn Reson Imaging*, **20**, 83-89, 2004.

[86] FW Wehrli and PK Saha, "Quantification of 3D Topology and Scale of Trabecular Bone in the Limited Spatial Resolution Regime of in Vivo Micro-MRI," *Microscopy and Microanalysis*, **10**, 718-719, 2004.

[87] FW Wehrli, HK Song, PK Saha, and AC Wright, "Quantitative MRI for the assessment of bone structure and function," *NMR Biomed*, **19**, 731-64, 2006.

[88] FW Wehrli, GA Ladinsky, C Jones, M Benito, J Magland, B Vasilic, AM Popescu, B Zemel, AJ Cucchiara, AC Wright, HK Song, PK Saha, H Peachey, and PJ Snyder, "In vivo magnetic resonance detects rapid remodeling changes in the topology of the trabecular bone network after menopause and the protective effect of estradiol," *J Bone Miner Res*, **23**, 730-40, 2008, PubMed Central PMCID: PMC2674544.

[89] Z Xu, M Sonka, and PK Saha, "Improved tensor scale computation with application to medical image interpolation," *Comput Med Imaging Graph*, **35**, 64-80, 2011.

References .....*Continued*

[90] Y Xu, G Liang, G Hu, Y Yang, J Geng, and PK Saha, "Quantification of coronary arterial stenoses in CTA using fuzzy distance transform," *Computerized Medical Imaging and Graphics*, **36**, 11-24, 2012.

[91] Z Xu, PK Saha, and S Dasgupta, "Tensor scale: An analytic approach with efficient computation and applications," *Comput Vis Image Underst*, **116**, 1060-1075, 2012, PubMed Central PMCID: PMC4519998.

[92] Y Zhuge, JK Udupa, and PK Saha, "Vectorial scale-based fuzzy connected image segmentation," *Computer Vision and Image Understanding*, **101**, 177-193, 2006.

Acknowledgments

Collaborators

Steven M. Levy, Eric Hoffman, Trudy L. Burns, Richard Shields, Chadi A. Calarge, James C. Torner, Laurie M. McCormick, Ravi Regatte, X. Edward Guo, Felix W. Wehrli, Robin Strand, Filip Malberg, Ingela Nystrom, Yung Kong, Gunilla Borgefors, Jayaram K Udupa, Chris Ciesielski

Scientists/Post-doctoral Fellows/Engineers

Guoyuan Liang, Duan Hong, Subhadip Basu, Jamuna Kanta Singh, Ryan Amelon, Zhiyun Gao

Graduate Students

Zhiyun Gao, Yinxiao Liu, Ziyue Xu, Yan Xu, Cheng Li
Dakai Jin, Cheng Chen, Xiaoliu Zhang, Syed Nadeem Ahmed

Grant Acknowledgments

- NIH R01 AR054439 (PI: Saha)
- ICTS/CTSA pilot grant (PI: Saha)
- NIH R01 AR051376 (Sub-contract PI: Saha; Columbia University)
- NIH R01 AR056260 (Sub-contract PI: Saha; New York University)
- NIH R01 DE012101-13S1 (PI: Levy)
- NIH R01 HD062507 (PI: Shields)
- NIH R01 HL-064368 (PI: Hoffman)

THANK YOU!